International Journal of Robotics and Control Systems
Vol. 5, No. 5, 2025, pp. 2546-2567
ISSN 2775-2658
http://pubs2.ascee.org/index.php/ijrcs

Parametric Eigen-space Characterization via Static Output Feedback in MIMO Control Systems: A New Look to Output Feedback Gain Matrix Design for Turbo-Generator System

Belkacem Bekhiti [a,1], Kamel Hariche [a,2], Jamshed Iqbal [b,3], and Abdel-Nasser Sharkawy [c,d,4,*]

[a] Institute of Aeronautics and Space Studies, (IASS), University of Blida 1 BP 270 Blida (09000), Algeria
[b] School of Digital and Physical Sciences, Faculty of Science and Engineering, University of Hull, Hull HU6 7RX, UK
[c] Mechanical Engineering Department, Faculty of Engineering, Qena University, Qena 83523, Egypt
[d] Mechanical Engineering Department, College of Engineering, Fahad Bin Sultan University, Tabuk 47721, Saudi Arabia
[1] belkacem1988@hotmail.co.uk; [2] khariche@yahoo.com; [3] J.Iqbal@hull.ac.uk; [4] abdelnassersharkawy@eng.svu.edu.eg
* Corresponding Author

ARTICLE INFO

Article history
Received June 30, 2025
Revised August 03, 2025
Accepted November 20, 2025

Keywords
Block forms;
Eigenspace Characterization;
Output feedback;
MIMO systems;
Multivariable Control Systems;
Parameterization

ABSTRACT

This paper presents a novel parametric output feedback strategy for MIMO control systems, enabling full closed-loop eigenvalue assignment through structured transformations without relying on prior state feedback or restrictive assumptions. The method uses a sector matrix to capture spectral characteristics of the closed-loop system and employs a convex LMI-based optimization framework for feedback gain computation. Its performance is validated on a benchmark turbo-generator system characterized by large scale and tightly coupled dynamics. Compared to conventional techniques such as adaptive pole placement and eigenstructure assignment, which often involve high control effort, sensitivity to disturbances, or limited precision, the proposed approach delivers superior results. It achieves significantly lower steady-state errors (RMSE: 0.013 and 0.009), minimal control input magnitudes (maximum of: 14.12 and 3.12 for the two inputs), reduced spectral sensitivity (2.12), and improved robustness to eigenvalue perturbations (relative variation 0.018). These findings underscore the method's practical applicability, computational efficiency, and robustness, making it a strong candidate for high-performance MIMO control applications.

1. Introduction

Induction The problem of eigenvalue assignment in multivariable (MIMO) control systems via static output feedback (SOF) has long attracted attention due to its practical importance in robust, optimal, and adaptive control design. Early foundational studies established the theoretical bounds on pole placement using output feedback [1]–[3], showing that up to min (m, p) eigenvalues can be arbitrarily placed, where m and p are the numbers of system inputs and outputs, respectively. Unlike state feedback, which requires full state measurement, SOF offers a more realistic solution in practice by relying solely on measurable outputs. Significant research efforts have focused on necessary and sufficient conditions for eigenvalue assignment feasibility, including approaches based on algebraic geometry and structural properties of system matrices [4]–[6]. This led to deeper characterizations of the SOF problem space [7,8], and the development of numerical methods that handle both parametric and non-parametric formulations [9]–[12]. Methods relying on eigenstructure assignment, modal matrix construction, and companion form transformations have been explored for several decades [13]–[16]. Notable advances include robust pole placement via gradient flows [17,18], and optimization-based feedback synthesis [9,10], [19], with further refinements proposed in block-structure relocation and matrix polynomial formulations [20]–[23].

Despite these developments, SOF design remains inherently nonlinear and non-convex. Traditional iterative algorithms often require precise initial estimates or impose structural constraints, limiting their scalability to high-dimensional systems [24]–[27]. In response, hybrid analytical–numerical methods have been introduced to improve stability, tractability, and robustness under uncertainty [28]–[32]. More recently, the integration of artificial intelligence and learning-based optimization has offered promising new avenues for output feedback control. For instance, reinforcement learning has been used to construct adaptive controllers with reduced computational complexity [33], while neural networks enable dynamic gain tuning in uncertain environments [34,35]. Techniques such as Physics-Informed Neural Networks (PINNs) and event-triggered observers have further extended applicability to real-time MIMO systems [36]–[39].

In addition, convexification strategies have been introduced to approximate non-convex SOF design problems using linear matrix inequalities (LMIs), as seen in recent works on control synthesis under structured uncertainties [40]–[42]. These innovations have been validated in diverse application domains, including robotics [31,34], machines and aerospace [43]–[45], biomedical systems [46], and energy systems [47,48]. Motivated by these trends, this work presents a new parametric formulation for output feedback design that enables full eigenvalue assignment without prior state feedback. The approach uses block similarity transformations and sector matrices to derive an explicit analytical expression for the SOF gain matrix. This leads to a structured nonlinear system capturing all feasible solutions. Unlike iterative or optimization-based methods, the proposed approach improves transparency, reduces computational effort, and ensures strong numerical stability in practice. The main contributions and novelties are summarized as follows:

- An optimal static output feedback algorithm has been developed for multivariable systems.
- Projection of the entire space into the allowable space through the LMI optimization algorithm
- The proposed SOF control technique is applied to a turbo-generator system.

The remainder of the paper is organized as follows: Section 2 outlines the theoretical background that shows the impact of operator theory on linear systems and Eigen-space decomposition. It reviews relevant algebraic structures and system transformations. Section 3 introduces the proposed methodology and presents its parametric formulation. Section 4 validates the approach through two case studies on benchmark systems. Section 5 compares the turbo-generator case study, with two methods reported in the literature. Finally, Section 6 concludes this study and highlights the future perspectives.

2. Theoretical Foundations and Operator-Theoretic Foundations

This section provides the mathematical foundation for the proposed method, introducing operator-theoretic concepts, rational matrix-valued functions, and spectral projectors. These tools are essential for analyzing multivariable systems and designing structured output feedback controllers. The eigenspace decomposition and projector-based techniques define the spectral structure of the closed-loop system. High-order differential systems (*polynomial operators*) often involve large-dimensional matrices, which has led to a renewed interest in rational matrix polynomial and state-space representations [49]. Polynomial systems theory relies on the properties of polynomials and polynomial matrices, using *polynomial operator algebra* (i.e., a natural extension of classical operational calculus based on Laplace and z-transforms). To clarify these concepts, consider finite-dimensional Hilbert spaces $\boldsymbol{\mathcal{U}}$,$\boldsymbol{\mathcal{Y}}$ representing the *input* and *output* spaces, respectively. Consider the *differential operator* $\lambda = d/dt$, understood as an unbounded densely defined closed linear operator on a suitable domain $\boldsymbol{\mathcal{D}}(\lambda) \subset L^2(\mathbb{R}, \boldsymbol{\mathcal{U}})$, generating a strongly continuous semigroup on L^2. Defining two operator-valued matrix polynomials: $\boldsymbol{D}_L(\lambda) = \sum_{i=0}^{\ell} \boldsymbol{D}_{Li}\lambda^{\ell-i} \in \boldsymbol{\mathcal{B}}(\boldsymbol{\mathcal{Y}})$, $\boldsymbol{N}_L(\lambda) = \sum_{i=0}^{\ell} \boldsymbol{N}_{Li}\lambda^{\ell-i} \in \boldsymbol{\mathcal{B}}(\boldsymbol{\mathcal{U}},\boldsymbol{\mathcal{Y}})$ where $\boldsymbol{D}_{Li} \in \mathbb{R}^{p\times p} \subset \boldsymbol{\mathcal{B}}(\boldsymbol{\mathcal{Y}})$, $\boldsymbol{N}_{Li} \in \mathbb{R}^{p\times m} \subset \boldsymbol{\mathcal{B}}(\boldsymbol{\mathcal{U}},\boldsymbol{\mathcal{Y}})$, and $\boldsymbol{\mathcal{B}}(.)$ denotes the space of bounded linear operators between corresponding spaces. Then the differential system can be formalized as an operator identity: $\boldsymbol{D}_L(\lambda)\mathbf{y}(\lambda) = \boldsymbol{N}_L(\lambda)\mathbf{u}(\lambda)$ with $\mathbf{u} \in \boldsymbol{\mathcal{D}}(\boldsymbol{N}_L(\lambda))$, $\mathbf{y} \in \boldsymbol{\mathcal{D}}(\boldsymbol{D}_L(\lambda))$, both contained in a suitable function space (e.g., Sobolev spaces $\mathcal{H}^{\ell}(\mathbb{R},\boldsymbol{\mathcal{U}})$, $\mathcal{H}^{\ell}(\mathbb{R},\boldsymbol{\mathcal{Y}})$). By applying the functional calculus for the differential operator λ, and assuming $\boldsymbol{D}_L(\lambda)$ is left-invertible in the ring of rational operator-valued functions, we obtain the input-output map: $\mathbf{y}(\lambda) = \boldsymbol{H}(\lambda)\mathbf{u}(\lambda)$ with $\boldsymbol{H}(\lambda) = \boldsymbol{D}_L^{-1}(\lambda)\boldsymbol{N}_L(\lambda)$ where $\boldsymbol{H}(\lambda) \in \boldsymbol{\mathcal{B}}(\boldsymbol{\mathcal{U}},\boldsymbol{\mathcal{Y}})$ is a rational matrix-valued function defined on a domain in the complex plane $\lambda \in \Upsilon \subset \mathbb{C}$. Alternatively, one may define a right matrix fraction description of $\boldsymbol{H}(\lambda)$ as: $\boldsymbol{H}(\lambda) = \boldsymbol{N}_R(\lambda)\boldsymbol{D}_R^{-1}(\lambda)$ where $\boldsymbol{D}_R(\lambda) = \sum_{i=0}^{\ell} \boldsymbol{D}_{Ri}\lambda^{\ell-i} \in \boldsymbol{\mathcal{B}}(\boldsymbol{\mathcal{U}})$, $\boldsymbol{N}_R(\lambda) = \sum_{i=0}^{\ell} \boldsymbol{N}_{Ri}\lambda^{\ell-i} \in \boldsymbol{\mathcal{B}}(\boldsymbol{\mathcal{U}},\boldsymbol{\mathcal{Y}})$. Such a rational operator-valued function $\boldsymbol{H}(\lambda)$ admits a *state-space realization* under the realization theory of infinite-dimensional linear systems.

Theorem 1 *Let* $\boldsymbol{\mathcal{U}},\boldsymbol{\mathcal{Y}},\boldsymbol{\mathcal{X}}$ *be finite-dimensional Hilbert spaces* (*e.g.,* $\mathbb{R}^m$; $\mathbb{R}^p$; $\mathbb{R}^n$) *and let the operator* $\boldsymbol{H}: \Upsilon \subset \mathbb{C} \to \boldsymbol{\mathcal{B}}(\boldsymbol{\mathcal{U}},\boldsymbol{\mathcal{Y}})$ *be a proper rational operator-valued function, analytic on a connected open set* $\Upsilon \subset \mathbb{C}$ *containing the resolvent set of some operator. Then, there exists a quadruple of bounded linear operator*s $(\boldsymbol{A},\boldsymbol{B},\boldsymbol{C},\boldsymbol{D}) \in \boldsymbol{\mathcal{B}}(\boldsymbol{\mathcal{X}}) \times \boldsymbol{\mathcal{B}}(\boldsymbol{\mathcal{U}},\boldsymbol{\mathcal{X}}) \times \boldsymbol{\mathcal{B}}(\boldsymbol{\mathcal{X}},\boldsymbol{\mathcal{Y}}) \times \boldsymbol{\mathcal{B}}(\boldsymbol{\mathcal{U}},\boldsymbol{\mathcal{Y}})$, *with*: $\boldsymbol{A}: \boldsymbol{\mathcal{X}} \to \boldsymbol{\mathcal{X}}$, $\boldsymbol{B}: \boldsymbol{\mathcal{U}} \to \boldsymbol{\mathcal{X}}$, $\boldsymbol{C}: \boldsymbol{\mathcal{X}} \to \boldsymbol{\mathcal{Y}}$ and $\boldsymbol{D} \in \boldsymbol{\mathcal{B}}(\boldsymbol{\mathcal{U}},\boldsymbol{\mathcal{Y}})$ *such that for all* $\lambda \in \rho(\boldsymbol{A})$ (*resolvent set of* $\boldsymbol{A}$), $\boldsymbol{H}(\lambda) = \boldsymbol{C}(\lambda\boldsymbol{I} - \boldsymbol{A})^{-1}\boldsymbol{B} + \boldsymbol{D}$ where $(\lambda\boldsymbol{I} - \boldsymbol{A})^{-1}$ *is the resolvent operator of* $\boldsymbol{A}$. *Moreover, the realization is minimal if*:

- span$\{\boldsymbol{A}^k\boldsymbol{B}\mathbf{u}\colon\ \mathbf{u} \in \boldsymbol{\mathcal{U}}, k \geq 0\}$ *is dense in* $\boldsymbol{\mathcal{X}}$ (*controllability*),
- span$\{\boldsymbol{C}\boldsymbol{A}^k\mathbf{x}\colon\ \mathbf{x} \in \boldsymbol{\mathcal{X}}, k \geq 0\}$ *is dense in* $\boldsymbol{\mathcal{Y}}$ (*observability*),

Specifically, there exist two canonical minimal realizations: $(\boldsymbol{A}_c,\boldsymbol{B}_c,\boldsymbol{C}_c,\boldsymbol{D}_c)$ and $(\boldsymbol{A}_o,\boldsymbol{B}_o,\boldsymbol{C}_o,\boldsymbol{D}_o)$ *called controllability and observability realizations* (*respectively*), *with*

$$\begin{Bmatrix} \boldsymbol{H}(\lambda) = \boldsymbol{N}_R(\lambda)\boldsymbol{D}_R^{-1}(\lambda) = \boldsymbol{C}_c(\lambda\boldsymbol{I} - \boldsymbol{A}_c)^{-1}\boldsymbol{B}_c + \boldsymbol{D}_c \\ = \boldsymbol{D}_L^{-1}(\lambda)\boldsymbol{N}_L(\lambda) = \boldsymbol{C}_o(\lambda\boldsymbol{I} - \boldsymbol{A}_o)^{-1}\boldsymbol{B}_o + \boldsymbol{D}_o \end{Bmatrix} \tag{1}$$

And

$$\boldsymbol{D}_R(\lambda) = \sum_{i=0}^{\ell} \boldsymbol{D}_{Ri}\lambda^{\ell-i};\ \boldsymbol{N}_R(\lambda) = \sum_{i=0}^{\ell} \boldsymbol{N}_{Ri}\lambda^{\ell-i};\ \boldsymbol{D}_L(\lambda) = \sum_{i=0}^{\ell} \boldsymbol{D}_{Li}\lambda^{\ell-i};\ \boldsymbol{N}_L(\lambda) = \sum_{i=0}^{\ell} \boldsymbol{N}_{Li}\lambda^{\ell-i}$$

Proof: We define a hierarchical sequence of abstract state variables $\{\mathbf{x}_i(\lambda)\}_{i=1}^{\ell} \subset \mathcal{H}$ where $\mathcal{H} = \mathcal{H}^{\ell}(\mathbb{R},\mathbb{R}^m)$ is the Sobolev space and each belonging to the image of resolvents of λ, by recursive relations derived from the inverse powers of λ. That is:

$$\mathbf{x}_1(\lambda) = \lambda^{-1}[\boldsymbol{N}_{L\ell}\mathbf{u}(\lambda) - \boldsymbol{D}_{L\ell}\mathbf{y}(\lambda)] \quad \dots \quad \mathbf{x}_{\ell}(\lambda) = \lambda^{-1}[\boldsymbol{N}_{L1}\mathbf{u}(\lambda) - \boldsymbol{D}_{L1}\mathbf{y}(\lambda) + \mathbf{x}_{\ell-1}(\lambda)]$$

After recursive substitution and rearrangement, the linear time-invariant (LTI) dynamics can be cast into a *first-order operator differential system*:

$$\left\{\begin{array}{l} \lambda\begin{bmatrix} \mathbf{x}_1(\lambda) \\ \vdots \\ \mathbf{x}_k(\lambda) \\ \vdots \\ \mathbf{x}_{\ell}(\lambda) \end{bmatrix} = \begin{bmatrix} \boldsymbol{O}_p & \cdots & \boldsymbol{O}_p & -\boldsymbol{D}_{L\ell} \\ \boldsymbol{I}_p & \cdots & \boldsymbol{O}_p & -\boldsymbol{D}_{L\ell-1} \\ \vdots & \vdots & \vdots & \vdots \\ \boldsymbol{O}_p & \cdots & \boldsymbol{O}_p & -\boldsymbol{D}_{L2} \\ \boldsymbol{O}_p & \cdots & \boldsymbol{I}_p & -\boldsymbol{D}_{L1} \end{bmatrix}\begin{bmatrix} \mathbf{x}_1(\lambda) \\ \vdots \\ \mathbf{x}_k(\lambda) \\ \vdots \\ \mathbf{x}_{\ell}(\lambda) \end{bmatrix} + \begin{bmatrix} \boldsymbol{N}_{L\ell} - \boldsymbol{D}_{L\ell}\boldsymbol{N}_{L0} \\ \vdots \\ \boldsymbol{N}_{L2} - \boldsymbol{D}_{L2}\boldsymbol{N}_{L0} \\ \boldsymbol{N}_{L1} - \boldsymbol{D}_{L1}\boldsymbol{N}_{L0} \end{bmatrix}\mathbf{u}(\lambda) \\ \mathbf{y}(\lambda) = \begin{bmatrix} \boldsymbol{O}_p & \cdots & \boldsymbol{O}_p & \boldsymbol{I}_p \end{bmatrix}\begin{bmatrix} \mathbf{x}_1(\lambda) \\ \vdots \\ \mathbf{x}_k(\lambda) \\ \vdots \\ \mathbf{x}_{\ell}(\lambda) \end{bmatrix} + \boldsymbol{N}_{L0}\mathbf{u}(\lambda) \end{array}\right\} \tag{2}$$

with $\boldsymbol{O}_p$ is a p^{th} order null matrix, $\boldsymbol{I}_p$ is a p^{th} order identity matrix.

More compactly this can be written as $\lambda\mathbf{x}_o(\lambda)=\boldsymbol{A}_o\mathbf{x}_o(\lambda)+\boldsymbol{B}_o\mathbf{u}(\lambda)$; $\mathbf{y}(\lambda)=\boldsymbol{C}_o\mathbf{x}_o(\lambda)+\boldsymbol{D}_o\mathbf{u}(\lambda)$ where

- $\mathbf{x}_o(t)\in\mathbb{R}^{\ell p}$ collects the auxiliary observable state variables,
- $\boldsymbol{A}_o\in\mathbb{R}^{\ell p\times\ell p}$ is an observable block companion-like matrix constructed from $\boldsymbol{D}_{Li}$,
- $\boldsymbol{B}_o\in\mathbb{R}^{\ell p\times m}$ encode the algebraic dependencies between input and auxiliary variables,
- $\boldsymbol{C}_o\in\mathbb{R}^{p\times\ell p}$ encode the algebraic dependencies between output and auxiliary variables,
- $\boldsymbol{D}_o=\boldsymbol{N}_{L0}$ is the direct feedthrough matrix.

Thus, the transfer function $\boldsymbol{H}(\lambda)\in\mathbb{R}(\lambda)^{p\times m}$ is given by:

$$\boldsymbol{H}(\lambda)=\boldsymbol{D}_L^{-1}(\lambda)\boldsymbol{N}_L(\lambda)=\boldsymbol{C}_o(\lambda\boldsymbol{I}-\boldsymbol{A}_o)^{-1}\boldsymbol{B}_o+\boldsymbol{D}_o.$$

Similarly, the system admits a right matrix fraction description $\mathbf{y}(\lambda)=\boldsymbol{N}_R(\lambda)\boldsymbol{D}_R^{-1}(\lambda)\mathbf{u}(\lambda)$, and

$$\mathbf{y}(\lambda)=\left\{\boldsymbol{N}_{R0}+\left[\sum_{i=1}^{\ell}[\boldsymbol{N}_{Ri}-\boldsymbol{N}_{R0}\boldsymbol{D}_{Ri}]\lambda^{\ell-i}\right]\left[\sum_{i=0}^{\ell}\boldsymbol{D}_{Ri}\lambda^{\ell-i}\right]^{-1}\right\}\mathbf{u}(\lambda)=\boldsymbol{N}_{R0}\mathbf{u}(\lambda)+\mathbf{y}_{\text{new}}(\lambda)$$

Let us rewrite this last equation in the following form:

$$\left[\sum_{i=1}^{\ell}[\boldsymbol{N}_{Ri}-\boldsymbol{N}_{R0}\boldsymbol{D}_{Ri}]\lambda^{\ell-i}\right]^{-1}\mathbf{y}_{\text{new}}(\lambda)=\left[\sum_{i=0}^{\ell}\boldsymbol{D}_{Ri}\lambda^{\ell-i}\right]^{-1}\mathbf{u}(\lambda)=\boldsymbol{Q}(\lambda)$$

This last equation gives $\lambda^{\ell}\boldsymbol{Q}(\lambda)=\mathbf{u}(\lambda)[\boldsymbol{D}_{R1}\lambda^{\ell-1}\boldsymbol{Q}(\lambda)+\boldsymbol{D}_{R2}\lambda^{\ell-2}\boldsymbol{Q}(\lambda)+\cdots+\boldsymbol{D}_{R\ell}\boldsymbol{Q}(\lambda)]$ and $\mathbf{y}_{\text{new}}(\lambda)=[\boldsymbol{N}_{R1}-\boldsymbol{N}_{R0}\boldsymbol{D}_{R1}]\lambda^{\ell-1}\boldsymbol{Q}(\lambda)+\cdots+[\boldsymbol{N}_{R\ell}-\boldsymbol{N}_{R0}\boldsymbol{D}_{R\ell}]\boldsymbol{Q}(\lambda)$. Now, we define a sequence of state variables: $\mathbf{x}_k(\lambda)=\lambda^{k-1}\boldsymbol{Q}(\lambda)$; where $k=1\ldots\ell$ and by recursive formulation we get $\lambda\mathbf{x}_1(\lambda)=\mathbf{x}_2(\lambda)$; $\lambda\mathbf{x}_2(\lambda)=\mathbf{x}_3(\lambda)$; …; $\lambda\mathbf{x}_\ell(\lambda)=\lambda^{\ell}\boldsymbol{Q}(\lambda)$ and the new output is given by the expression $\mathbf{y}_{\text{new}}(\lambda)=\boldsymbol{N}_{R0}\mathbf{u}(\lambda)+\sum_{i=1}^{\ell}[\boldsymbol{N}_{Ri}-\boldsymbol{N}_{R0}\boldsymbol{D}_{Ri}]\mathbf{x}_{\ell-i+1}(\lambda)$. It is very easy to check that: $\mathbf{x}_\ell(\lambda)=\lambda^{\ell-1}\boldsymbol{Q}(\lambda)=\mathbf{u}(\lambda)-\sum_{i=1}^{\ell}\boldsymbol{D}_{Ri}\mathbf{x}_{\ell+1-i}(\lambda)$ so, in matrix form we can write:

$$\left\{\begin{array}{l}\lambda\begin{bmatrix}\mathbf{x}_1(\lambda)\\ \vdots\\ \mathbf{x}_k(\lambda)\\ \vdots\\ \mathbf{x}_\ell(\lambda)\end{bmatrix}=\begin{bmatrix}\boldsymbol{O}_m & \boldsymbol{I}_m & \cdots & \boldsymbol{O}_m\\ \boldsymbol{O}_m & \boldsymbol{O}_m & \cdots & \boldsymbol{O}_m\\ \vdots & \vdots & \ldots & \boldsymbol{O}_m\\ \boldsymbol{O}_m & \boldsymbol{O}_m & \ldots & \boldsymbol{I}_m\\ -\boldsymbol{D}_{R\ell} & -\boldsymbol{D}_{R\ell-1} & \cdots & -\boldsymbol{D}_{R1}\end{bmatrix}\begin{bmatrix}\mathbf{x}_1(\lambda)\\ \vdots\\ \mathbf{x}_k(\lambda)\\ \vdots\\ \mathbf{x}_\ell(\lambda)\end{bmatrix}+\begin{bmatrix}\boldsymbol{O}_m\\ \vdots\\ \boldsymbol{O}_m\\ \boldsymbol{I}_m\end{bmatrix}\mathbf{u}(\lambda)\\ \mathbf{y}(\lambda)=[(\boldsymbol{N}_{R\ell}-\boldsymbol{N}_{R0}\boldsymbol{D}_{R\ell})\ \cdots\ (\boldsymbol{N}_{R1}-\boldsymbol{N}_{R0}\boldsymbol{D}_{R1})]\begin{bmatrix}\mathbf{x}_1(\lambda)\\ \vdots\\ \mathbf{x}_k(\lambda)\\ \vdots\\ \mathbf{x}_\ell(\lambda)\end{bmatrix}+\boldsymbol{N}_{R0}\mathbf{u}(\lambda)\end{array}\right\} \tag{3}$$

Or, more compactly $\lambda\mathbf{x}_c(\lambda)=\boldsymbol{A}_c\mathbf{x}_c(\lambda)+\boldsymbol{B}_c\mathbf{u}(\lambda)$; $\mathbf{y}(\lambda)=\boldsymbol{C}_c\mathbf{x}_c(\lambda)+\boldsymbol{D}_c\mathbf{u}(\lambda)$ where:

- $\mathbf{x}_c(t)\in\mathbb{R}^{\ell m}$ collects the auxiliary controllable state variables,
- $\boldsymbol{A}_c\in\mathbb{R}^{\ell m\times\ell m}$ is a controllable block companion-like matrix constructed from $\boldsymbol{D}_{Ri}$,
- $\boldsymbol{B}_c\in\mathbb{R}^{\ell m\times m}$ encode the algebraic dependencies between input and auxiliary variables,
- $\boldsymbol{C}_c\in\mathbb{R}^{p\times\ell m}$ encode the algebraic dependencies between output and auxiliary variables,
- $\boldsymbol{D}_c=\boldsymbol{N}_{R0}$ is the direct feedthrough matrix.

Thus, the transfer function $\boldsymbol{H}(\lambda)$ is obtained as:

$$\boldsymbol{H}(\lambda)=\boldsymbol{N}_R(\lambda)\boldsymbol{D}_R^{-1}(\lambda)=\boldsymbol{C}_c(\lambda\boldsymbol{I}-\boldsymbol{A}_c)^{-1}\boldsymbol{B}_c+\boldsymbol{D}_c$$

It is understood that the state space representation is not unique irrespective of the transfer matrix which is unique. This means that an infinity of state space representation should belong to the same system, due to the fact that any operator will have an infinite equivalent forms related by isomorphism. That is if we have $\lambda\mathbf{x}_1(t) = \boldsymbol{A}_1\mathbf{x}_1(\lambda) + \boldsymbol{B}_1\mathbf{u}(\lambda)$; $\mathbf{y}(\lambda) = \boldsymbol{C}_1\mathbf{x}_1(\lambda) + \boldsymbol{D}_1\mathbf{u}(\lambda)$ and $\mathbf{x}_1 = \boldsymbol{T}\mathbf{x}_2$ then $\lambda\mathbf{x}_2(t) = \boldsymbol{A}_2\mathbf{x}_2(\lambda) + \boldsymbol{B}_2\mathbf{u}(\lambda)$; $\mathbf{y}(\lambda) = \boldsymbol{C}_2\mathbf{x}_2(\lambda) + \boldsymbol{D}_2\mathbf{u}(\lambda)$ with $\boldsymbol{A}_2 = \boldsymbol{T}^{-1}\boldsymbol{A}_1\boldsymbol{T}$; $\boldsymbol{B}_2 = \boldsymbol{T}^{-1}\boldsymbol{B}_1$; $\boldsymbol{C}_2 = \boldsymbol{C}_1\boldsymbol{T}$; and $\boldsymbol{D}_2 = \boldsymbol{D}_1$. In term of transfer matrix, we have

$$\begin{aligned}\boldsymbol{H}(\lambda) = \boldsymbol{C}_2(\lambda\boldsymbol{I} - \boldsymbol{A}_2)^{-1}\boldsymbol{B}_2 + \boldsymbol{D}_2 &= \boldsymbol{C}_1\boldsymbol{T}(\lambda\boldsymbol{I} - \boldsymbol{T}^{-1}\boldsymbol{A}_1\boldsymbol{T})^{-1}\boldsymbol{T}^{-1}\boldsymbol{B}_1 + \boldsymbol{D}_1 \\ &= \boldsymbol{C}_1(\lambda\boldsymbol{I} - \boldsymbol{A}_1)^{-1}\boldsymbol{B}_1 + \boldsymbol{D}_1\end{aligned}$$

Hence, every finite-dimensional LTI system with polynomial differential representation admits both left and right matrix fraction descriptions in the ring of rational operator-valued functions $\mathbb{R}(\lambda)^{p\times m}$, and can be *realized canonically* in state-space form. (Q.E.D) □

Note: The ring $\mathbb{R}[\lambda]$ of real-coefficient polynomials can be naturally embedded in the ring of rational matrix functions $\mathbb{R}(\lambda)$, and the structure of $\boldsymbol{H}(\lambda)$ reflects its *fractional ideal* form in this ring, supporting a dual interpretation via left and right coprime factorizations.

Let $\sum = (\boldsymbol{A}, \boldsymbol{B}, \boldsymbol{C}, \boldsymbol{D})$ be a finite-dimensional LTI system defined over Hilbert spaces $\boldsymbol{\mathcal{X}} = \mathbb{R}^n$, $\boldsymbol{\mathcal{U}} = \mathbb{R}^m$, and $\boldsymbol{\mathcal{Y}} = \mathbb{R}^p$, governed by the state space evolution: $\lambda\mathbf{x}(\lambda) = \boldsymbol{A}\mathbf{x}(\lambda) + \boldsymbol{B}\mathbf{u}(\lambda)$ and $\mathbf{y}(\lambda) = \boldsymbol{C}\mathbf{x}(\lambda) + \boldsymbol{D}\mathbf{u}(\lambda)$ where $\boldsymbol{A} \in \boldsymbol{\mathcal{B}}(\boldsymbol{\mathcal{X}})$; $\boldsymbol{B} \in \boldsymbol{\mathcal{B}}(\boldsymbol{\mathcal{U}}, \boldsymbol{\mathcal{X}})$; $\boldsymbol{C} \in \boldsymbol{\mathcal{B}}(\boldsymbol{\mathcal{X}}, \boldsymbol{\mathcal{Y}})$; and $\boldsymbol{D} \in \boldsymbol{\mathcal{B}}(\boldsymbol{\mathcal{U}}, \boldsymbol{\mathcal{Y}})$.

Definition 1 *The system* $\sum$ *is said to be exactly controllable on the time interval* $[t_0, t_1]$ *if for every pair of states* $\mathbf{x}_0, \mathbf{x}_1 \in \boldsymbol{\mathcal{X}}$, *there exists a piecewise continuous control input* $\mathbf{u} \in L^2([t_0, t_1], \boldsymbol{\mathcal{U}})$ *such that the solution* $\mathbf{x}(t) \in C^1([t_0, t_1], \boldsymbol{\mathcal{X}})$ *of the system satisfies*: $\mathbf{x}(t_0) = \mathbf{x}_0,\ \mathbf{x}(t_1) = \mathbf{x}_1$.

Definition 2 *The system* $\sum$ *is said to be exactly observable on the time interval* $[t_0, t_1]$ *if for any* $\mathbf{x}_0 \in \boldsymbol{\mathcal{X}}$, *the knowledge of the output trajectory* $\mathbf{y} \in \boldsymbol{\mathcal{Y}}$ *for* $t \in [t_0, t_1]$, *corresponding to zero input* $\mathbf{u}(t) = \mathbf{0}$, *allows for the unique determination of the initial condition* $\mathbf{x}(t_0) = \mathbf{x}_0$.

To formally characterize exact controllability/observability in finite-dimensional LTI systems, the following theorem provides necessary and sufficient algebraic and analytical conditions.

Theorem 2 (Kalman's Rank Condition) *The controllability Gramians of linear system is given by integral formula* $\mathbf{W}_c(0, t_1) = \int_0^{t_1} \left[e^{-\boldsymbol{A}\tau}\boldsymbol{B}\boldsymbol{B}^\top e^{-\boldsymbol{A}^\top\tau}\right] d\tau$ *and the controllability matrix is given by* $\boldsymbol{\Omega}_c = [\boldsymbol{B}\ \ \boldsymbol{A}\boldsymbol{B}\ \cdots\ \boldsymbol{A}^{n-1}\boldsymbol{B}\,] \in \mathbb{R}^{n\times nm}$. *The necessary and sufficient condition for the linear time invariant system to be completely state-controllable is given by one of the following condition*:

(i) $\mathbf{W}_c(0, t_1)$ *is nonsingular, or equivalently* $\mathbf{W}_c(0, t_1)$ *is positive definite (PD) matrix.*
(ii) *The matrix* $\boldsymbol{\Omega}_c$ *is full rank*, i.e., $\mathrm{rank}(\boldsymbol{\Omega}_c) = n$. *Or equivalently* $\boldsymbol{\Omega}_c\boldsymbol{\Omega}_c^\top$ *is nonsingular.*

The observability Gramians of linear system is given by $\mathbf{W}_o(0, t_1) = \int_0^{t_1} \left[e^{-\boldsymbol{A}^\top\tau}\boldsymbol{C}^\top\boldsymbol{C}e^{-\boldsymbol{A}\tau}\right] d\tau$ *and the observability matrix is* $\boldsymbol{\Omega}_o^\top = \left[\boldsymbol{C}^\top\ \ \boldsymbol{C}^\top\boldsymbol{A}^\top\ \cdots\ \boldsymbol{C}^\top(\boldsymbol{A}^{n-1})^\top\,\right] \in \mathbb{R}^{n\times nm}$. *The necessary and sufficient condition for the LTIsystem to be completely state-observable is given by one of*:

(i) $\mathbf{W}_o(0, t_1)$ *is nonsingular, or equivalently* $\mathbf{W}_o(0, t_1)$ *is positive definite (PD) matrix.*
(ii) *The matrix* $\boldsymbol{\Omega}_o$ *is full rank*, i.e., $\mathrm{rank}(\boldsymbol{\Omega}_o\,) = n$. *Or equivalently* $\boldsymbol{\Omega}_o^\top\boldsymbol{\Omega}_o$ *is nonsingular.*

Proof: see [16], [49].

Without loss of generality, setting $t_0 = 0$ and $\mathbf{x}(t_1) = \mathbf{0}$, the system is *completely controllable* if for every $\mathbf{x}_0 \in \boldsymbol{\mathcal{X}}$, there exists an input $\mathbf{u} \in L^2([0, t_1], \boldsymbol{\mathcal{U}})$ such that the corresponding trajectory satisfies $\mathbf{x}(t_1) = \mathbf{0}$. A necessary and sufficient condition for complete controllability is the surjectivity of the controllability map: $\boldsymbol{\mathcal{C}}_{[0,t_1]}: L^2([0, t_1], \boldsymbol{\mathcal{U}}) \to \boldsymbol{\mathcal{X}}, \boldsymbol{u} \longmapsto \int_0^{t_1} e^{\boldsymbol{A}(t_1-\tau)}\boldsymbol{B}\mathbf{u}(\tau)d\tau$. In algebraic terms, this is equivalent to Kalman's rank condition: $\mathrm{rank}[\boldsymbol{B}\ \ \boldsymbol{A}\boldsymbol{B} \cdots \boldsymbol{A}^{n-1}\boldsymbol{B}\,] = n$.

The observability of the system is equivalent to the injectivity of the *observability operator*: $\boldsymbol{\mathcal{O}}_{[t_0,t_1]}: \boldsymbol{\mathcal{X}} \to L^2([t_0, t_1], \boldsymbol{\mathcal{Y}})$, $\boldsymbol{x}_o \longmapsto \boldsymbol{C}e^{\boldsymbol{A}t}\boldsymbol{B}\mathbf{x}_0$. In other words, the system is observable if $\boldsymbol{\mathcal{O}}_{[t_0,t_1]}(\mathbf{x}_0) = \mathbf{0} \implies \mathbf{x}_0 = \mathbf{0}$. That is, the state can be recovered uniquely from the output measurement over the time interval. In algebraic form, the system is observable if and only if the observability matrix satisfies: $\mathrm{rank}\big[\boldsymbol{C}^\top \;\; \boldsymbol{C}^\top\boldsymbol{A}^\top \; \cdots \; \boldsymbol{C}^\top(\boldsymbol{A}^{n-1})^\top\big] = n$.

Theorem 3 (Popov-Belevitch-Hautus Test [49]) *Given an LTI system described by its state space evolution* $\lambda\mathbf{x}(\lambda) = \boldsymbol{A}\mathbf{x}(\lambda) + \boldsymbol{B}\mathbf{u}(\lambda)$; and $\mathbf{y}(\lambda) = \boldsymbol{C}\mathbf{x}(\lambda) + \boldsymbol{D}\mathbf{u}(\lambda)$ *then, the two tests for controllability are*:

- *PBH Rank Test*: *The pair* $(\boldsymbol{A},\boldsymbol{B})$ *is controllable iff* $\mathrm{rank}[\lambda\boldsymbol{I} - \boldsymbol{A},\ \boldsymbol{B}] = n$ *for any* $\lambda \in \sigma(\boldsymbol{A})$
- *PBH Eigenvector Test*: $(\boldsymbol{A},\boldsymbol{B})$ *is controllable iff there exists no left eigenvector of* $\boldsymbol{A}$ *orthogonal to the columns of* $\boldsymbol{B}$, *or* $(\boldsymbol{A},\boldsymbol{B})$ *is controllable* $\Leftrightarrow \{\mathbf{w}^\top\boldsymbol{A} = \lambda\mathbf{w}^\top \text{ and } \mathbf{w}^\top\boldsymbol{B} = \mathbf{0}\}$ *only if* $\mathbf{w} = \mathbf{0}$.

The two Popov-Belevitch-Hautus tests for observability are:

- *PBH Rank Test*: *The pair* $(\boldsymbol{A},\boldsymbol{C})$ *is observable iff* $\mathrm{rank}\big[\lambda\boldsymbol{I} - \boldsymbol{A}^\top,\ \boldsymbol{C}^\top\big]^\top = n$ *for any* $\lambda \in \sigma(\boldsymbol{A})$
- *PBH Eigenvector Test*: $(\boldsymbol{A},\boldsymbol{C})$ *is observable iff there exists no right eigenvector of* $\boldsymbol{A}$ *orthogonal to the columns of* $\boldsymbol{C}$, *or* $(\boldsymbol{A},\boldsymbol{C})$ *is observable* $\Leftrightarrow \{\boldsymbol{A}\mathbf{v} = \lambda\mathbf{v} \text{ and } \boldsymbol{C}\mathbf{v} = \mathbf{0}\}$ *only if* $\mathbf{v} = \mathbf{0}$.

If $\mathrm{rank}(\boldsymbol{\Omega}_c) = r < n$, then the system is not fully controllable: the reachable subspace $\boldsymbol{\mathcal{R}} := \mathrm{Im}\,(\boldsymbol{\Omega}_c) \subset \boldsymbol{\mathcal{X}}$ has dimension r, and only the projection of $\mathbf{x}(t)$ onto $\boldsymbol{\mathcal{R}}$ can be arbitrarily steered via control. it is not possible to move from $\mathbf{x}_0$ to any arbitrary final state $\mathbf{x}_1$, i.e., only r entries of the state can be moved arbitrary and the remaining ones moves with its own dynamics (not assigned by the control law). If the system is stabilizable there is a similarity transformation (due to E.R. KALMAN) that decomposes the system in controllable and non-controllable parts. The set of all controllable states $\boldsymbol{\mathcal{X}}_c$, named the *controllable subspace*, is given by:

$$\boldsymbol{\mathcal{X}}_c = \left\{\mathbf{x} \,\middle|\; \mathbf{x} = -\int_0^{t_1} e^{\boldsymbol{A}(t_1-\tau)}\boldsymbol{B}\mathbf{u}(\tau)d\tau,\ \ \forall\ \mathbf{u}(\tau)\right\}$$

Corollary 1 [16] *The necessary and sufficient condition for partial state* $\boldsymbol{\eta}$ *of the system to be controllable is*: $\boldsymbol{\eta} \in \boldsymbol{\mathcal{X}}_c = \boldsymbol{\mathcal{R}}(\boldsymbol{\Omega}_c)$, *where* $\boldsymbol{\mathcal{R}}(\boldsymbol{\Omega}_c) = \{\mathbf{x} \in \boldsymbol{\mathcal{X}} |\ \ \mathbf{x} = \boldsymbol{\Omega}_c\mathbf{v},\ \ \forall\ \mathbf{v} \in \mathbb{R}^{nm}\}$ *is the range space of the matrix* $\boldsymbol{\Omega}_c$.

If we can find an input $\mathbf{u}(t)$ that is able to transfer the output $\mathbf{y}(t)$ of the continuous LTI system from any arbitrary position to zero in a finite time t, then the system is said to be completely *output controllable.*

Theorem 4 (Complete output-controllability) *The necessary and sufficient condition for the linear time invariant system to be completely output-controllable is given by one of the following condition*:

(i) $\mathbf{W}_{oc}(0,t_1) = \int_0^{t_1}\left[\boldsymbol{C}e^{-\boldsymbol{A}\tau}\boldsymbol{B}\boldsymbol{B}^\top e^{-\boldsymbol{A}^\top\tau}\boldsymbol{C}^\top\right]d\tau$ *is nonsingular,* $\Leftrightarrow \mathbf{W}_{oc}(0,t_1)$ *is PD matrix.*

(ii) *The* $\boldsymbol{\Omega}_{oc} = [\boldsymbol{C}\boldsymbol{B} \,\vdots\, \boldsymbol{C}\boldsymbol{A}\boldsymbol{B} \cdots \vdots\, \boldsymbol{C}\boldsymbol{A}^{n-1}\boldsymbol{B} \,\vdots\, \boldsymbol{D}] \in \mathbb{R}^{p\times(n+1)m}$ *is full row rank,* i.e., $\mathrm{rank}\,\boldsymbol{\Omega}_{oc} = p$.

Proof: see [20]–[29].

Note: The controllability, observability, and cross Gramians are indeed characterized as solutions to algebraic matrix equations, specifically Lyapunov or Sylvester equations. The controllability Gramian $\mathbf{W}_c$ satisfies the dual Lyapunov equation: $\mathbf{W}_c\boldsymbol{A}^\top + \boldsymbol{A}\mathbf{W}_c + \boldsymbol{B}\boldsymbol{B}^\top = \mathbf{0}$. The observability Gramian $\mathbf{W}_o$ satisfies the dual Lyapunov equation: $\boldsymbol{A}^\top\mathbf{W}_o + \mathbf{W}_o\boldsymbol{A} + \boldsymbol{C}^\top\boldsymbol{C} = \mathbf{0}$.

2.1. Eigen-Space Decomposition and Projectors

The eigen-space decomposition of a matrix $\boldsymbol{A}$ along its spectral projectors leads to powerful insights, particularly in control theory, model reduction, and frequency-domain analysis. Let $\boldsymbol{A} \in \mathbb{C}^{n\times n}$ be a diagonalizable matrix. Then there exists a complete set of *spectral projectors* $\{\boldsymbol{E}_i\}_{i=1}^k$ corresponding to its distinct eigenvalues $\{\lambda_i\}_{i=1}^k$, such that: $\boldsymbol{A} = \sum_{i=1}^k \lambda_i\boldsymbol{E}_i$ with $\boldsymbol{E}_i\boldsymbol{E}_j = \delta_{ij}\boldsymbol{E}_i$, $\sum_{i=1}^k \boldsymbol{E}_i = \boldsymbol{I}$ and each projector $\boldsymbol{E}_i$ satisfies: $\boldsymbol{E}_i^2 = \boldsymbol{E}_i$, and $\boldsymbol{E}_i\boldsymbol{A} = \boldsymbol{A}\boldsymbol{E}_i = \lambda_i\boldsymbol{E}_i$. This gives the *spectral decomposition* of $\boldsymbol{A}$ in terms of its eigen-subspaces: $\mathbb{C}^n = \bigoplus_{i=1}^k \mathrm{Im}(\boldsymbol{E}_i)$. If $\boldsymbol{A}$ is not diagonalizable, we generalize the decomposition using *Dunford's decomposition*: $\boldsymbol{A} = \boldsymbol{A}_d + \boldsymbol{N}$ where $\boldsymbol{A}_d = \sum_{i=1}^{k} \lambda_i \boldsymbol{E}_i$, $\boldsymbol{N} = \sum_{i=1}^{k} \boldsymbol{N}_i$ and $\boldsymbol{A}_d \boldsymbol{N} - \boldsymbol{N}\boldsymbol{A}_d = \boldsymbol{0}$ with $\boldsymbol{N}_i$ nilpotent operators acting on the generalized eigenspaces [50,52]. Now, let's explore how spectral projectors are constructed from left and right eigenvectors of $\boldsymbol{A}$. Assume that $\boldsymbol{A} \in \mathbb{C}^{n\times n}$ and suppose $\lambda_i \in \mathbb{C}$ is a simple eigenvalue of $\boldsymbol{A}$. Then: $\boldsymbol{A}\mathbf{v}_i = \lambda_i \mathbf{v}_i$ and $\mathbf{w}_i^{\top}\boldsymbol{A} = \lambda_i \mathbf{w}_i^{\top}$ where $\mathbf{v}_i, \mathbf{w}_i^{\top}$ are right/left eigenvectors of $\boldsymbol{A}$. We can normalize them such that: $\mathbf{w}_i^{\top}\mathbf{v}_i = 1$ and therefore $\boldsymbol{A}\left[\sum_{i=1}^{k} \mathbf{v}_i \mathbf{w}_i^{\top}\right] = \sum_{i=1}^{k} \lambda_i \mathbf{v}_i \mathbf{w}_i^{\top}$ but $\sum_{i=1}^{k} \mathbf{v}_i \mathbf{w}_i^{\top} = \boldsymbol{I}$, hence $\boldsymbol{E}_i = \mathbf{v}_i \mathbf{w}_i^{\top}$. Also, we have $\boldsymbol{A}[\mathbf{v}_1 \dots \mathbf{v}_n] = [\mathbf{v}_1 \dots \mathbf{v}_n]\mathrm{diag}(\lambda_1 \dots \lambda_n)$ or equivalently, $\boldsymbol{AV} = \boldsymbol{V\Lambda}$. If we put $\boldsymbol{W} = \boldsymbol{V}^{-1}$ then $\boldsymbol{A} = \boldsymbol{V\Lambda W}$. If $\boldsymbol{A}$ is diagonalizable but eigenvalues are repeated, and let $\{\mathbf{v}_{ij}\}$ be a basis of right eigenvectors associated with λ_j, and $\{\mathbf{w}_{ij}\}$ be the dual left eigenvectors, then $\boldsymbol{E}_j = \sum_{i=1}^{r} \mathbf{v}_{ij}\mathbf{w}_{ij}^{\top}$. In light of this, consider the multivariable LTI system described by the transfer matrix, defined as:

$$\boldsymbol{H}(\lambda) = \boldsymbol{N}(\lambda)\boldsymbol{D}(\lambda)^{-1} = \boldsymbol{C}(\lambda\boldsymbol{I} - \boldsymbol{A})^{-1}\boldsymbol{B} + \boldsymbol{D} = \boldsymbol{CV}(\lambda\boldsymbol{I} - \boldsymbol{\Lambda})^{-1}\boldsymbol{WB} + \boldsymbol{D} \tag{4}$$

where

$\boldsymbol{A} \in \mathbb{R}^{n\times n}$; $\boldsymbol{B} \in \mathbb{R}^{n\times m}$; $\boldsymbol{C} \in \mathbb{R}^{p\times n}$; $\boldsymbol{D} \in \mathbb{R}^{p\times m}$
$\mathbf{v}_i$: Right eigenvector of $\boldsymbol{A}$
$\mathbf{w}_i$: Left eigenvector of $\boldsymbol{A}$
λ_i : The eigenvalues of $\boldsymbol{A}$
$\boldsymbol{V} = [\mathbf{v}_1 \quad \mathbf{v}_2 \quad \cdots \quad \mathbf{v}_n]$; $\boldsymbol{W} = \boldsymbol{V}^{-1}$

$$\boldsymbol{W} = \begin{bmatrix} \mathbf{w}_1^{\top} \\ \mathbf{w}_2^{\top} \\ \vdots \\ \mathbf{w}_n^{\top} \end{bmatrix}; \qquad \boldsymbol{\Lambda} = \begin{bmatrix} \lambda_1 & \cdots & 0 \\ \vdots & \ddots & \vdots \\ 0 & \cdots & \lambda_n \end{bmatrix}$$

Expressing the transfer function in terms of its eigenvalues (i.e. assume that matrix $\boldsymbol{D}$ is non-zero):

$$\boldsymbol{H}(\lambda) = \sum_{i=1}^{n} \frac{\boldsymbol{C}\mathbf{v}_i\mathbf{w}_i^{\top}\boldsymbol{B}}{\lambda - \lambda_i} + \boldsymbol{D} = \frac{\boldsymbol{H}_1}{\lambda - \lambda_1} + \cdots + \frac{\boldsymbol{H}_n}{\lambda - \lambda_n} + \boldsymbol{D} \tag{5}$$

with: $\boldsymbol{H}_i = \boldsymbol{C}\mathbf{v}_i\mathbf{w}_i^{\top}\boldsymbol{B} = [(\lambda - \lambda_i)(\boldsymbol{H}(\lambda) - \boldsymbol{D})]_{\lambda=\lambda_i}$. If $\boldsymbol{A} \in \mathbb{R}^{n\times n}$ is diagonalizable then can be rewritten as:

$$\boldsymbol{A} = \boldsymbol{V\Lambda W} = \sum_{i=1}^{n} \lambda_i \mathbf{v}_i \mathbf{w}_i^{\top} \quad \text{and} \quad \boldsymbol{H}_i = \boldsymbol{C}\boldsymbol{E}_i\boldsymbol{B} \tag{6}$$

The partial fraction expansion of $\boldsymbol{H}(\lambda)$, show that each mode λ_i contributes a rank-one (or low-rank) residue $\boldsymbol{H}_i = \boldsymbol{C}\boldsymbol{E}_i\boldsymbol{B}$ to the total transfer behavior. Each term $\boldsymbol{H}_i/(\lambda - \lambda_i)$ represents the modal response associated with eigenvalue λ_i. The rank and norm of $\boldsymbol{H}_i$ quantify the contribution of mode λ_i to input-output behavior.

2.2. Block Canonical Forms of MIMO Systems

Consider an LTI system represented by the state equation in general coordinates:

$$\dot{\mathbf{x}}(t) = \boldsymbol{A}\mathbf{x}(t) + \boldsymbol{B}\mathbf{u}(t) \quad \text{and} \quad \mathbf{y}(t) = \boldsymbol{C}\mathbf{x}(t) + \boldsymbol{D}\mathbf{u}(t) \tag{7}$$

where $\mathbf{x} \in \mathbb{R}^{n}$, $\mathbf{y} \in \mathbb{R}^{p}$, $\mathbf{u} \in \mathbb{R}^{m}$, $\boldsymbol{A} \in \mathbb{R}^{n\times n}$, $\boldsymbol{B} \in \mathbb{R}^{n\times m}$, and $\boldsymbol{C} \in \mathbb{R}^{p\times n}$.

Definition 3 *The system described by equation* (7) *is said to be block controllable of index* ℓ *if the matrix* $\boldsymbol{\Omega}_c = \mathrm{row}\left(\boldsymbol{A}^i\boldsymbol{B}\right)_{i=0}^{\ell-1}$ *has full rank and* $\ell = n/m$ *is an integer. In this context the operation* $\mathrm{row}(\boldsymbol{X}_i)_{i=0}^{\ell-1}$ *is the row-wise concatenation of the matrices* $\boldsymbol{X}_i$ *for* $i = 0,1,\dots,\ell-1$, *interpreted as building a matrix by aligning those matrices horizontally from left to right.*

Next theorem gives conditions under which a multivariable linear system can be transformed into a block controller canonical form. This structure simplifies control design and analysis. The transformation is possible if the system order is divisible by the input dimension and the system is block controllable of the corresponding index.

Theorem 5 (I. Gohberg and B. Bekhiti [22,23]) *The multivariable control system described in (7) can be transformed into a block controller form if the following two conditions are satisfied*:

① $\ell = n/m$ *is an integer*
② *The system is nlock controllable of index* ℓ

If both conditions are met, then the coordinate transformation $\mathbf{x}_c(t) = \boldsymbol{T}_c\mathbf{x}(t)$ *transforms the system into the following block canonical controller form*

$$\dot{\mathbf{x}}_c(t) = \boldsymbol{A}_c\mathbf{x}_c(t) + \boldsymbol{B}_c\mathbf{u}(t) \quad \text{and} \quad \mathbf{y}(t) = \boldsymbol{C}_c\mathbf{x}_c(t) + \boldsymbol{D}_c\mathbf{u}(t) \tag{8}$$

where: $\boldsymbol{T}_c = \operatorname{col}\left(\boldsymbol{T}_{c1}\boldsymbol{A}^i\right)_{i=0}^{\ell-1}$; $\boldsymbol{T}_{c1} = [\boldsymbol{O}_m \vdots \boldsymbol{O}_m \vdots \cdots \vdots \boldsymbol{I}_m]\left(\operatorname{row}\left(\boldsymbol{A}^i\boldsymbol{B}\right)_{i=0}^{\ell-1}\right)^{-1}$ *and*

$$\left\{\boldsymbol{A}_c = \boldsymbol{T}_c\boldsymbol{A}\boldsymbol{T}_c^{-1} = \begin{bmatrix} \boldsymbol{O}_m & \boldsymbol{I}_m & \cdots & \boldsymbol{O}_m \\ \boldsymbol{O}_m & \boldsymbol{O}_m & \cdots & \boldsymbol{O}_m \\ \vdots & \vdots & \dots & \boldsymbol{O}_m \\ \boldsymbol{O}_m & \boldsymbol{O}_m & \dots & \boldsymbol{I}_m \\ -\boldsymbol{A}_\ell & -\boldsymbol{A}_{\ell-1} & \cdots & -\boldsymbol{A}_1 \end{bmatrix}; \quad \boldsymbol{B}_c = \boldsymbol{T}_c\boldsymbol{B} = \begin{bmatrix} \boldsymbol{O}_m \\ \boldsymbol{O}_m \\ \vdots \\ \boldsymbol{I}_m \end{bmatrix}; \quad \boldsymbol{C}_c = \boldsymbol{C}\boldsymbol{T}_c^{-1} = \begin{bmatrix} \boldsymbol{C}_\ell^\top \\ \vdots \\ \boldsymbol{C}_2^\top \\ \boldsymbol{C}_1^\top \end{bmatrix}^\top\right\}$$

with: $\mathbf{x}_c \in \mathbb{R}^n$, $\boldsymbol{A}_i \in \mathbb{R}^{m\times m}$, $\boldsymbol{C}_i \in \mathbb{R}^{p\times m}$, $i = 1,.,\ell$, $\boldsymbol{I}_m$ and $\boldsymbol{O}_m$ *are the* $m \times m$ *identity and null matrices respectively, and the superscript* $\top$ *denote the transpose. In this context the operation* $\operatorname{col}(\boldsymbol{X}_i)_{i=0}^{\ell-1}$ *is the column-wise concatenation of the matrices* $\boldsymbol{X}_i$ for $i = 0,1,\dots,\ell-1$, *interpreted as building a matrix by aligning them vertically from top to down.* □

Let $\boldsymbol{R}_i \in \mathbb{R}^{m\times m}$ be a square matrices (called *right block roots* or *solvents*) such that the right functional evaluation of $\sum_{k=0}^{\ell}\boldsymbol{A}_k\boldsymbol{R}_i^{\ell-k} = \boldsymbol{O}_m$ or $[\boldsymbol{A}_\ell \dots \boldsymbol{A}_1\ \boldsymbol{A}_0]\operatorname{col}\left(\boldsymbol{R}_i^k\right)_{k=0}^{\ell}$ for $i = 1,2,\dots,\ell$. In matrix form we can write $\boldsymbol{A}_c\boldsymbol{X}_i = \boldsymbol{X}_i\boldsymbol{R}_i$ where $\boldsymbol{X}_i = \operatorname{col}\left(\boldsymbol{R}_i^k\right)_{k=0}^{\ell-1}$. If we define the right block Vandermonde matrix $\boldsymbol{V}_R = [\boldsymbol{X}_1\ \boldsymbol{X}_2 \dots \boldsymbol{X}_\ell]$ then $\boldsymbol{A}_c\boldsymbol{V}_R = \boldsymbol{V}_R\boldsymbol{\Lambda}_R$ with $\boldsymbol{\Lambda}_R = \operatorname{blkdiag}(\boldsymbol{R}_1 \dots \boldsymbol{R}_\ell)$.

Definition 4 *The system described by equation* (7) *is said to be block observable of index* ℓ *if the matrix* $\boldsymbol{\Omega}_o = \operatorname{col}\left(\boldsymbol{C}\boldsymbol{A}^i\right)_{i=0}^{\ell-1}$ *has full rank and* $\ell = n/m$ *is an integer.*

Theorem 6 (I. Gohberg and B. Bekhiti [22,23]) *Consider the multivariable system described by innovation equation (7). This system can be expressed in block observable canonical form if the following two criteria are met*:

① *The ratio* $\ell = n/p$ *is a positive integer and*
② *The system satisfies block observability of index* ℓ, *i.e., the block observability matrix* $\boldsymbol{\Omega}_o$ *has full rank. Under these conditions, the system admits a similarity transformation of the form* $\mathbf{x}_o(t) = \boldsymbol{T}_o\mathbf{x}(t)$, *where* $\boldsymbol{T}_o$ *is a nonsingular transformation matrix. This yields an equivalent state-space representation in block observable canonical form*

$$\dot{\mathbf{x}}_o(t) = \boldsymbol{A}_o\mathbf{x}_o(t) + \boldsymbol{B}_o\mathbf{u}(t) \quad \text{and} \quad \mathbf{y}(t) = \boldsymbol{C}_o\mathbf{x}_o(t) + \boldsymbol{D}_o\mathbf{u}(t) \tag{9}$$

where $\boldsymbol{T}_o = \operatorname{row}\left(\boldsymbol{A}^i\boldsymbol{T}_{o1}\right)_{i=0}^{\ell-1}$; $\boldsymbol{T}_{o1} = \left(\operatorname{col}\left(\boldsymbol{C}\boldsymbol{A}^i\right)_{i=0}^{\ell-1}\right)^{-1}[\boldsymbol{O}_p \vdots \boldsymbol{O}_p \vdots \cdots \vdots \boldsymbol{I}_p]^\top$ *and*

$$\left\{\boldsymbol{A}_o = \boldsymbol{T}_o^{-1}\boldsymbol{A}\boldsymbol{T}_o = \begin{bmatrix} \boldsymbol{O}_p & \cdots & \boldsymbol{O}_p & -\boldsymbol{A}_\ell \\ \boldsymbol{I}_p & \cdots & \boldsymbol{O}_p & -\boldsymbol{A}_{\ell-1} \\ \vdots & \vdots & \vdots & \vdots \\ \boldsymbol{O}_p & \cdots & \boldsymbol{O}_p & -\boldsymbol{A}_2 \\ \boldsymbol{O}_p & \cdots & \boldsymbol{I}_p & -\boldsymbol{A}_1 \end{bmatrix}; \quad \boldsymbol{B}_c = \boldsymbol{T}_o^{-1}\boldsymbol{B} = \begin{bmatrix} \boldsymbol{B}_\ell \\ \vdots \\ \boldsymbol{B}_2 \\ \boldsymbol{B}_1 \end{bmatrix}; \quad \boldsymbol{C}_o = \boldsymbol{C}\boldsymbol{T}_o = \begin{bmatrix} \boldsymbol{O}_p \\ \boldsymbol{O}_p \\ \vdots \\ \boldsymbol{I}_p \end{bmatrix}^\top\right\}$$

with $\mathbf{x}_o \in \mathbb{R}^n$, $\boldsymbol{A}_i \in \mathbb{R}^{p\times p}$, $\boldsymbol{B}_i \in \mathbb{R}^{p\times m}, i = 1,.,\ell$, $\boldsymbol{I}_p$ and $\boldsymbol{O}_p$ *are the* $p \times p$ *identity and null matrices respectively.* □

3. Eigen-Space Characterization and Key Findings

In multivariable linear systems, state feedback assigns closed-loop eigenvalues by shaping the matrix $\boldsymbol{A}-\boldsymbol{BK}$ to achieve desired dynamics. For fully controllable systems with full-state access, any pole configuration is achievable. When only outputs are measurable, output feedback can indirectly assign a subset of poles. Advanced methods like block pole placement generalize eigenvalue assignment by targeting invariant subspaces or matrix polynomial factors, allowing structured control in MIMO systems. In such systems with state dimension $n = \ell m$, the block controllable canonical form facilitates block pole assignment, where the gain matrix $\boldsymbol{K}$ is designed so that the closed-loop matrix $\boldsymbol{A}_d$ yields the desired characteristic matrix polynomial $\boldsymbol{D}_d(\lambda)$ [28].

3.1. Relocation of Block Poles via State Feedback

This subsection revisits the classical problem of closed-loop eigenvalue assignment via full state feedback. It establishes the block pole relocation framework, which is later extended to the output feedback setting. The relocation of block poles via state feedback in MIMO systems can be rigorously formulated as the spectral shaping of a bounded linear operator $\boldsymbol{A} \in \boldsymbol{\mathcal{B}}(\boldsymbol{\mathcal{X}})$ on a finite-dimensional Hilbert space $\boldsymbol{\mathcal{X}} \cong \mathbb{R}^n$, perturbed by the rank-m operator $\boldsymbol{BK} \in \boldsymbol{\mathcal{B}}(\boldsymbol{\mathcal{X}})$, where $\boldsymbol{B} \in \boldsymbol{\mathcal{B}}(\boldsymbol{\mathcal{X}},\boldsymbol{\mathcal{U}})$, $\boldsymbol{K} \in \boldsymbol{\mathcal{B}}(\boldsymbol{\mathcal{U}},\boldsymbol{\mathcal{X}})$, and $\boldsymbol{\mathcal{U}} \cong \mathbb{R}^m$ [13]. For systems admitting a block controllable realization with $\dim(\boldsymbol{\mathcal{X}}) = \ell m$, the problem reduces to synthesizing $\boldsymbol{K}$ such that the spectrum of the closed-loop operator $\boldsymbol{A}_d = \boldsymbol{A}-\boldsymbol{BK}$ matches a prescribed set of invariant factors encoded by a right matrix polynomial $\boldsymbol{D}_d(\lambda) \in \mathbb{R}[\lambda]^{m\times m}$. This constitutes a nontrivial inverse spectral problem in the algebra of rational operator-valued functions, constrained by block structural compatibility and requiring the transformability (via similarity) of a system of endomorphisms on $\boldsymbol{\mathcal{X}}$ [21].

Theorem 7 (B. Bekhiti [20]) *Let* $\sum = (\boldsymbol{A},\boldsymbol{B},\boldsymbol{C},\boldsymbol{D})$ *be a finite-dimensional linear time-invariant system defined over Hilbert spaces* $\boldsymbol{\mathcal{X}} \cong \mathbb{R}^n$, $\boldsymbol{\mathcal{U}} \cong \mathbb{R}^m$, *and* $\boldsymbol{\mathcal{Y}} \cong \mathbb{R}^p$, *admitting a rational transfer function representation*: $\boldsymbol{H}(\lambda) = \boldsymbol{C}(\lambda\boldsymbol{I}-\boldsymbol{A})^{-1}\boldsymbol{B}+\boldsymbol{D} = \boldsymbol{N}(\lambda)\boldsymbol{D}(\lambda)^{-1}$ *with* $\boldsymbol{N}(\lambda) \in \mathbb{R}[\lambda]^{p\times m}$ *and* $\boldsymbol{D}(\lambda) \in \mathbb{R}[\lambda]^{m\times m}$. *Assume the system is block controllable with* $n = \ell m$ *be a desired monic matrix polynomial whose set of right invariant factors (block poles) is* $\{\boldsymbol{R}_1, \dots, \boldsymbol{R}_\ell\} \subset \mathbb{C}^{m\times m}$. *Then, there exists a state feedback operator* $\boldsymbol{K} \in \boldsymbol{\mathcal{B}}(\boldsymbol{\mathcal{U}},\boldsymbol{\mathcal{X}})$ *such that the spectrum of the closed-loop operator* $\boldsymbol{A}_d = \boldsymbol{A}-\boldsymbol{BK}$ *satisfies the condition*: $\det\big(\boldsymbol{D}_d(\lambda)\big) = \det\big(\lambda\boldsymbol{I}-(\boldsymbol{A}-\boldsymbol{BK})\big)$ *with the feedback operator* $\boldsymbol{K}$ *given by*:

$$\boldsymbol{K} = \left[\boldsymbol{B}_c^{\top}\left(\mathrm{row}\big(\boldsymbol{A}^i\boldsymbol{B}\big)_{i=0}^{\ell-1}\right)^{-1}\boldsymbol{A}^{\ell}\right] - \mathrm{row}\big(\boldsymbol{R}_i^{\ell}\big)_{i=1}^{\ell}\left[\mathrm{row}\left(\mathrm{col}\big(\boldsymbol{R}_i^{k}\big)_{k=0}^{\ell-1}\right)_{i=1}^{\ell}\right]^{-1}\boldsymbol{T}_c \tag{10}$$

with $\boldsymbol{T}_c = \left\{\mathrm{col}\left(\boldsymbol{B}_c^{\top}\left(\mathrm{row}\big(\boldsymbol{A}^i\boldsymbol{B}\big)_{i=0}^{\ell-1}\right)^{-1}\boldsymbol{A}^i\right)_{i=0}^{\ell-1}\right\}$; *and* $\boldsymbol{B}_c^{\top} = [\boldsymbol{O}_m \vdots \boldsymbol{O}_m \vdots \cdots \vdots \boldsymbol{I}_m] \in \mathbb{R}^{m\times\ell m}$. *This construction yields a similarity transformation under which the closed-loop operator admits the prescribed spectral structure governed by* $\boldsymbol{D}_d(\lambda)$, *completing the block pole relocation.* □

The MIMO deterministic systems are described by the quadruple $\sum = (\boldsymbol{A},\boldsymbol{B},\boldsymbol{C},\boldsymbol{D})$. An observer $\widehat{\sum}$ is an auxiliary system evolving on the same state space $\boldsymbol{\mathcal{X}}$, with its state $\hat{\mathbf{x}}(t) \in \boldsymbol{\mathcal{X}}$ converging asymptotically to the true state $\mathbf{x}(t)$, regardless of the input $\mathbf{u}(t) \in \boldsymbol{\mathcal{U}}$. This convergence is governed by the observer error $\boldsymbol{\varepsilon}(t) := \mathbf{x}(t) - \hat{\mathbf{x}}(t)$ which follows a homogeneous system under the perturbed operator $\boldsymbol{A}-\boldsymbol{LC}$. The observer gain $\boldsymbol{L} \in \boldsymbol{\mathcal{B}}(\boldsymbol{\mathcal{Y}},\boldsymbol{\mathcal{X}})$ is designed to assign the spectrum of $\boldsymbol{A}-\boldsymbol{LC}$. When the pair $(\boldsymbol{A},\boldsymbol{C})$ is block observable and $\dim(\boldsymbol{\mathcal{X}}) = \ell p$, $\boldsymbol{L}$ can be synthesized so that the block eigenstructure of $\boldsymbol{A}-\boldsymbol{LC}$ matches any admissible monic matrix polynomial with prescribed right block roots [29].

Theorem 8 (B. Bekhiti [20]) *Let* $\sum = (\boldsymbol{A},\boldsymbol{B},\boldsymbol{C},\boldsymbol{D})$ *be a finite-dimensional linear time-invariant system described by:* $\dot{\mathbf{x}}(t) = \boldsymbol{A}\mathbf{x}(t) + \boldsymbol{B}\mathbf{u}(t)$; $\mathbf{y}(t) = \boldsymbol{C}\mathbf{x}(t) + \boldsymbol{D}\mathbf{u}(t)$ *with* $\mathbf{x}(t) \in \boldsymbol{\mathcal{X}}$ *and* $\dim(\boldsymbol{\mathcal{X}}) = \ell p$ *and assume that the pair* $(\boldsymbol{A},\boldsymbol{C})$ *is block observable. Then there exists an observer gain* $\boldsymbol{L} \in \mathbb{R}^{n\times p}$ *such that the spectrum of the error dynamics operator* $\boldsymbol{A} - \boldsymbol{LC}$ *matches a prescribed set of block roots* $\{\boldsymbol{S}_1,\dots,\boldsymbol{S}_\ell\} \subset \mathbb{C}^{p\times p}$*, if and only if* $(\boldsymbol{A},\boldsymbol{C})$ *admits a block observable realization. The gain matrix* $\boldsymbol{L}$ *is given explicitly by*:

$$\boldsymbol{L} = \left[\boldsymbol{A}^{\ell}\left(\mathrm{col}\left(\boldsymbol{C}\boldsymbol{A}^{i}\right)_{i=0}^{\ell-1}\right)^{-1}\boldsymbol{C}_o^{\top}\right] - \boldsymbol{T}_o\left[\mathrm{col}\left(\mathrm{row}\left(\boldsymbol{S}_i^{k}\right)_{k=0}^{\ell-1}\right)_{i=1}^{\ell}\right]^{-1}\left(\mathrm{col}\left(\boldsymbol{S}_i^{\ell}\right)_{i=1}^{\ell}\right) \tag{11}$$

with $\boldsymbol{T}_o = \mathrm{row}\left(\boldsymbol{A}^{i}\left(\mathrm{col}\left(\boldsymbol{C}\boldsymbol{A}^{i}\right)_{i=0}^{\ell-1}\right)^{-1}\boldsymbol{C}_o^{\top}\right)_{i=0}^{\ell-1}$; *and* $\boldsymbol{C}_o = \left[\boldsymbol{O}_p \vdots \boldsymbol{O}_p \vdots \cdots \vdots \boldsymbol{I}_p\right] \in \mathbb{R}^{p\times \ell p}$. *If* $\boldsymbol{A} - \boldsymbol{LC}$ *is Hurwitz, then* $\varepsilon(t) \to 0$ *as* $t \to \infty$*, and the estimate* $\hat{\mathbf{x}}(t)$ *converges asymptotically to the true state* $\mathbf{x}(t)$*, independently of initial conditions. And the observer evolution is given by the following state equation* $\dot{\hat{\mathbf{x}}}(t) = (\boldsymbol{A} - \boldsymbol{LC})\hat{\mathbf{x}}(t) + [\boldsymbol{B} \vdots \boldsymbol{L}]\left[\mathbf{u}^{\top}(t)\ \ \mathbf{y}^{\top}(t)\right]^{\top}$. □

3.2. The Proposed Output Feedback Gain Matrix Design

This subsection presents the core contribution of the paper. Building on the theoretical foundations of Section 2, it formulates a robust parametric output feedback method for structured pole placement in finite-dimensional MIMO systems without requiring full state measurement. The method leverages operator-theoretic representations of the closed-loop dynamics, Kronecker-algebraic parameterization, and similarity transformations based on block controllability and observability. A sector matrix is introduced to encapsulate the dominant spectral content within a sensitive subspace, and Theorem 9 establishes the use of LMI-based optimization to compute the output feedback gain matrix explicitly. This structured approach ensures closed-loop stability under both algebraic and geometric constraints and enables efficient and scalable implementation [49].

Assume now that the feedforward term satisfies $\boldsymbol{D} = \boldsymbol{0}$, and define the first Markov parameter as $\boldsymbol{M}_1 = \sum_{i=1}^{n}\lambda_i\boldsymbol{H}_i = \boldsymbol{C}[\lambda_1\boldsymbol{E}_1 + \cdots + \lambda_n\boldsymbol{E}_n]\boldsymbol{B} = \boldsymbol{CAB}$. Suppose further that $\boldsymbol{H}(\lambda)$ is an $m \times m$ matrix, implying that the product $\boldsymbol{CB}$ is square. Under this condition, we may represent the expression accordingly

$$\boldsymbol{H}(\lambda) = \sum\nolimits_{i=1}^{n}\left(\frac{\boldsymbol{C}\boldsymbol{E}_i\boldsymbol{B}}{\lambda - \lambda_i}\right) \tag{12}$$

Therefore, if $\boldsymbol{A}_d$ denotes the target closed-loop matrix to be matched through state feedback $\mathbf{u} = -\boldsymbol{K}\mathbf{x}$, then:

$$\sum\nolimits_{i=1}^{n}\lambda_i\boldsymbol{H}_{id} = \boldsymbol{C}\boldsymbol{A}_d\boldsymbol{B} \Rightarrow \left(\boldsymbol{B}^{\top}\otimes\boldsymbol{C}\right)\mathrm{vec}(\boldsymbol{A}_d) = \mathrm{vec}\left(\sum\nolimits_{i=1}^{n}\lambda_i\boldsymbol{H}_{id}\right) \tag{13}$$

Here, $\otimes$ denotes the Kronecker product, and vec(•) represents the vectorization operator. Given that under state feedback the closed-loop matrix is $\boldsymbol{A}_d = \boldsymbol{A} - \boldsymbol{BK}$, we can express this relation in terms of $\boldsymbol{K}$ as follows:

$$\left(\boldsymbol{B}^{\top}\otimes\boldsymbol{I}\right)\mathrm{vec}(\boldsymbol{K}) = \mathrm{vec}\left[(\boldsymbol{CB})^{-1}\left(\boldsymbol{CAB} - \sum\nolimits_{i=1}^{n}\lambda_i\boldsymbol{H}_{id}\right)\right] \tag{14}$$

Put differently, fact 1 can be interpreted as asserting that:

$$\left(\boldsymbol{B}^{\top}\otimes\boldsymbol{I}\right)\mathrm{vec}(\boldsymbol{K}) = \mathrm{vec}\left((\boldsymbol{CB})^{-1}(\boldsymbol{CAB} - \boldsymbol{C}\boldsymbol{A}_d\boldsymbol{B})\right) = \mathrm{vec}\left((\boldsymbol{CB})^{-1}(\boldsymbol{M}_1 - \boldsymbol{M}_{1d})\right) \tag{15}$$

Rather than applying state feedback, let us consider the output feedback control law defined by $\mathbf{u} = -\boldsymbol{K}\mathbf{y}$. In this case, the resulting target matrix is $\boldsymbol{A}_d = \boldsymbol{A} - \boldsymbol{BKC}$, and fact 2 can thus be reformulated accordingly:

$$\begin{aligned}(\boldsymbol{C}^{\top}\otimes\boldsymbol{B})\mathrm{vec}(\boldsymbol{K}) = \mathrm{vec}(\boldsymbol{A}-\boldsymbol{A}_d) \Rightarrow \mathrm{rank}(\boldsymbol{C}^{\top}\otimes\boldsymbol{B}) \\ \geq \mathrm{rank}([\boldsymbol{C}^{\top}\otimes\boldsymbol{B} \vdots \mathrm{vec}(\boldsymbol{A}-\boldsymbol{A}_d)])\end{aligned} \tag{16}$$

Definition 4 *The system described by the quadruple* $\sum = (\boldsymbol{A},\boldsymbol{B},\boldsymbol{C},\boldsymbol{D})$ *is referred to as non-defective if the system matrix* $\boldsymbol{A}$ *is non-defective, meaning that* $\boldsymbol{A}$ *has a diagonal Jordan form.*

Non-defective systems are highly desirable, as the poles of such systems exhibit less sensitivity to perturbations in system parameters (see Guangbin Cai in [42]). In order to obtain a non-defective closed-loop system, the matrix $\boldsymbol{\Lambda} = \mathrm{diag}(\lambda_1,\lambda_2,\cdots,\lambda_n)$ is selected as the Jordan canonical form of the desired matrix $\boldsymbol{A}_d = \boldsymbol{A}-\boldsymbol{BKC}$, where each λ_i $(i = 1,2,\cdots,n)$ denotes a prescribed complex-conjugate eigenvalue intended for the closed-loop system.

Remark: The computation of the output feedback matrix corresponding to a given triple $(\boldsymbol{B},\boldsymbol{A},\boldsymbol{C})$ can be approached through several algorithmic techniques. In this work, we propose a direct algebraic formulation based on the explicit structure of the closed-loop characteristic polynomial. This leads to an efficient and original parametric design methodology that utilizes a tailored state-space transformation to construct a complete parameterization of admissible output feedback matrices.

Notably, because the matrix $\boldsymbol{K}$ is affected from the left by $\boldsymbol{C}$ and from the right by $\boldsymbol{B}$, the method naturally facilitates the application of both block controllability and observability transformations from the outset. This yields an original framework for reconstructing the output feedback matrix. By applying a pre-multiplication on the left by $\boldsymbol{T}_c$ and on the right by $\boldsymbol{T}_o$, the output feedback equation transforms into:

$$\boldsymbol{BKC} = \boldsymbol{A}-\boldsymbol{A}_d \ \Rightarrow\ \boldsymbol{T}_c\boldsymbol{BKCT}_o = \boldsymbol{T}_c(\boldsymbol{A}-\boldsymbol{A}_d)\boldsymbol{T}_o \tag{17}$$

Based on the previously defined transformations $\boldsymbol{T}_c$, $\boldsymbol{T}_o$, and the matrices $\boldsymbol{B}_c$, $\boldsymbol{C}_o$, we derive the expression:

$$\boldsymbol{B}_c\boldsymbol{K}\boldsymbol{C}_o = \begin{bmatrix}\boldsymbol{O}_m\\ \vdots\\ \boldsymbol{I}_m\end{bmatrix}[\boldsymbol{O}_p \cdots \boldsymbol{K}] = \boldsymbol{T}_c(\boldsymbol{A}-\boldsymbol{A}_d)\boldsymbol{T}_o \ \Rightarrow\ \begin{bmatrix}\boldsymbol{0} & \boldsymbol{0}\\ \boldsymbol{0} & \boldsymbol{K}\end{bmatrix} = \boldsymbol{T}_c(\boldsymbol{A}-\boldsymbol{A}_d)\boldsymbol{T}_o = \boldsymbol{\Delta}_{co} \tag{18}$$

Therefore, the output feedback matrix can be constructed as: $\boldsymbol{K} = \boldsymbol{\Delta}_{co}(n-m+1{:}n, n-p+1{:}n)$

Question: What condition on the structure of $\boldsymbol{A}_d$ ensures that the system achieves the desired performance? To answer this, we perform the transformation $\boldsymbol{A}_{co} = \boldsymbol{T}_c\boldsymbol{A}\boldsymbol{T}_o$ and follow the procedure outlined below

$$\boldsymbol{A}_{co} = \left[\mathrm{col}\left\{\boldsymbol{B}_c^{\top}\left[\mathrm{row}\{\boldsymbol{A}^i\boldsymbol{B}\}_{i=0}^{\ell-1}\right]^{-1}\boldsymbol{A}^i\right\}_{i=0}^{\ell-1}\boldsymbol{A}\right]\mathrm{row}\left\{\boldsymbol{A}^i\left[\mathrm{col}\{\boldsymbol{C}\boldsymbol{A}^i\}_{i=0}^{\ell-1}\right]^{-1}\boldsymbol{C}_o^{\top}\right\}_{i=0}^{\ell-1} = \begin{bmatrix}\boldsymbol{A}_\alpha & \boldsymbol{A}_\beta\\ \boldsymbol{A}_\gamma & \boldsymbol{A}_\delta\end{bmatrix} \tag{19}$$

Using equation (19) it can be concluded that the desired closed-loop matrix can be parameterized in terms of $\boldsymbol{T}_c, \boldsymbol{T}_o, \boldsymbol{A}_\alpha, \boldsymbol{A}_\beta$ and $\boldsymbol{A}_\gamma$ as follows:

$$\boldsymbol{A}_d = \boldsymbol{T}_c^{-1}\begin{bmatrix}\boldsymbol{A}_\alpha & \boldsymbol{A}_\beta\\ \boldsymbol{A}_\gamma & \boldsymbol{A}_{sec}\end{bmatrix}\boldsymbol{T}_o^{-1} \tag{20}$$

where: $\boldsymbol{A}_{sec}$: denotes the sector matrix to be determined, and the submatrices are extracted as

$$\begin{aligned}\boldsymbol{A}_\alpha &= \boldsymbol{A}_{co}(1{:}(n-m), 1{:}(n-p)); & \boldsymbol{A}_\beta &= \boldsymbol{A}_{co}(1{:}(n-m), (n-p+1){:}n);\\ \boldsymbol{A}_\gamma &= \boldsymbol{A}_{co}((n-m+1){:}n, 1{:}(n-p)); & \boldsymbol{A}_\delta &= \boldsymbol{A}_{co}((n-m+1){:}n, (n-p+1){:}n)\end{aligned}$$

Remark: It should be emphasized that the matrix $\boldsymbol{A}_{sec}$ plays a central role in defining the closed-loop behavior, as it encapsulates all spectral characteristics of the system. Since it is the sole component that modifies the eigenspace of the closed-loop configuration, this sector structure is both critical and highly sensitive within the proposed design methodology.

$$\boldsymbol{\Delta}_{co} = \begin{bmatrix} \mathbf{0} & \mathbf{0} \\ \mathbf{0} & \boldsymbol{K} \end{bmatrix} \Rightarrow \boldsymbol{K} = \boldsymbol{A}_{\delta} - \boldsymbol{A}_{sec} \tag{21}$$

where: $\boldsymbol{K} \in \mathbb{R}^{m\times p}$, $\boldsymbol{A}_{\delta} \in \mathbb{R}^{m\times p}$ and $\boldsymbol{A}_{sec} \in \mathbb{R}^{m\times p}$.

The proposed approach imposes no constraints on the location or multiplicity of the eigenvalues and does not rely on any prior knowledge of the open-loop spectrum. Its core objective is to construct a parameterization of the target-matrix $\boldsymbol{A}_d$ as a function of $\boldsymbol{A}_{sec}$, such that:

$$\boldsymbol{A}_d = \boldsymbol{T}_c^{-1} \begin{bmatrix} \boldsymbol{A}_{\alpha} & \boldsymbol{A}_{\beta} \\ \boldsymbol{A}_{\gamma} & \boldsymbol{A}_{sec}(\boldsymbol{\theta}) \end{bmatrix} \boldsymbol{T}_o^{-1} = \mathbf{F}(\boldsymbol{\theta}); \qquad \boldsymbol{\theta} \in \mathbb{R}^{mp} \tag{22}$$

Where $\boldsymbol{A}_{sec}(\boldsymbol{\theta}) \in \mathbb{R}^{m\times p}$, $\mathbf{F}(\boldsymbol{\theta}) \in \mathbb{R}^{n\times n}$ and $\boldsymbol{\theta}$ represents the set of parameters defining the functional matrix $\boldsymbol{A}_{sec}(\boldsymbol{\theta})$, which must be identified to ensure that $\boldsymbol{A}_d$ achieves the desired spectral properties. In other words, if $\lambda_{d1}, \cdots, \lambda_{dn}$ denote the target closed-loop poles to be assigned through output feedback, then:

$$\left\{\begin{array}{rcc} \boldsymbol{\Delta}(\lambda) = & & \det\left(\lambda \boldsymbol{I} - \mathbf{F}(\boldsymbol{\theta})\right) \\ = & & (\lambda - \lambda_{d1})(\lambda - \lambda_{d2})\cdots(\lambda - \lambda_{dn}) \\ = & & \lambda^n + \alpha_1\lambda^{n-1} + \cdots + \alpha_n \end{array}\right\} \tag{23}$$

Applying the LMI-based convex optimization method, the solutions to a system of n equations with mp decision parameters $\boldsymbol{\theta}$ is obtained. LMI-based formulation allows for convex optimization, numerical robustness, and guarantees on feasibility, especially in the context of spectral assignment under structural constraints.

Theorem 9 *Let* $\sum = (\boldsymbol{A}, \boldsymbol{B}, \boldsymbol{C}, \boldsymbol{D})$ *be a finite-dimensional linear system that is both block controllable and block observable and let* $\boldsymbol{T}_c, \boldsymbol{T}_o \in GL_n(\mathbb{R})$ *be the associated similarity transformations. Suppose we define the closed-loop matrix via the parameterized form:* $\boldsymbol{A}_d = \boldsymbol{T}_c^{-1}[\boldsymbol{A}_{\alpha} \quad \boldsymbol{A}_{\beta};\ \boldsymbol{A}_{\gamma} \quad \boldsymbol{A}_{sec}(\boldsymbol{\theta})]\boldsymbol{T}_o^{-1} = \mathbf{F}(\boldsymbol{\theta})$; *where* $\boldsymbol{A}_{sec}(\boldsymbol{\theta}) \in \mathbb{R}^{m\times p}$ *is the sector matrix depending linearly on* $\boldsymbol{\theta} \in \mathbb{R}^{mp}$, *and all other blocks are fixed. Assume that the desired spectrum* $\sigma_d = \{\lambda_{d1}, \dots, \lambda_{dn}\} \subset \mathbb{C}^-$ *lies in the open left-half plane. Then, there exists a symmetric positive definite matrix* $\boldsymbol{P} \in \mathbb{R}^{n\times n}$ *such that the following Linear Matrix Inequality holds:* $\boldsymbol{F}(\boldsymbol{\theta})^{\top}\boldsymbol{P} + \boldsymbol{P}\boldsymbol{F}(\boldsymbol{\theta}) \prec 0$ *and the output feedback gain matrix* $\boldsymbol{K}(\boldsymbol{\theta}) := \boldsymbol{A}_{\delta} - \boldsymbol{A}_{sec}(\boldsymbol{\theta})$ *stabilizes the closed-loop system:* $\boldsymbol{A} - \boldsymbol{B}\boldsymbol{K}(\boldsymbol{\theta})\boldsymbol{C} = \boldsymbol{A}_d(\boldsymbol{\theta})$. *The design reduces to the convex feasibility problem: Find* $\boldsymbol{\theta} \in \mathbb{R}^{mp}$, $\boldsymbol{P} \in \mathbb{S}_{++}^n$ *such that* $\boldsymbol{F}(\boldsymbol{\theta})^{\top}\boldsymbol{P} + \boldsymbol{P}\boldsymbol{F}(\boldsymbol{\theta}) \prec 0$. *The matrix* $\boldsymbol{K}(\boldsymbol{\theta})$*can be computed by solving the following Linear Matrix Inequality (LMI) optimization problem:*

$$\left\{\begin{array}{ll} \text{minimize} & \operatorname{trace}(\boldsymbol{P}) \\ \text{subject to} & \boldsymbol{P} \succ 0, \quad \boldsymbol{F}(\boldsymbol{\theta})^{\top}\boldsymbol{P} + \boldsymbol{P}\boldsymbol{F}(\boldsymbol{\theta}) \prec 0. \end{array}\right\} \tag{24}$$

Solving this convex program yields a good choice of the sector matrix $\boldsymbol{A}_{sec}(\boldsymbol{\theta})$, *and thus an output feedback gain* $\boldsymbol{K}(\boldsymbol{\theta})$ *such that the closed-loop system: is asymptotically stable.* □

While the proposed method enables full eigenvalue assignment without state feedback, marking a major step in static output feedback design, its applicability is subject to certain conditions. It requires the system to be block controllable and block observable, as detailed in Theorems 5 to 9. These structural properties are necessary for the use of similarity transformations and sector matrix parameterization. In systems lacking such block structures or with deficient controllability/observability ranks, the LMI formulation may not yield feasible solutions. Additionally, in ill-conditioned or weakly coupled systems, eigenvalue placement may become sensitive, requiring careful tuning or regularization. Although theoretically scalable, very high-dimensional systems may face numerical issues unless sparsity or decomposition methods are applied. Future work may consider extending the approach to dynamic output feedback and observer-based frameworks to address these limitations.

Algorithm:
```
• Test system for block controllability and block observability      \\ Verify structural condition
• Derive the similarity isomorphisms $T_c$ and $T_o$                    \\ Use theorems 5 and 6
• Compute canonical form $A_{co}$ and reconstruct the matrix $A_\delta$    \\ Form transformed system
• Define $A_d$ through $\mathrm{F}(\theta)$ parameterization              \\ Define desired dynamics.
• Impose $\Delta(\lambda) = \det(\lambda I - \mathrm{F}(\theta))$ and solve via LMI
  minimize trace($P$); subject to $P \succ 0, F(\theta)^\top P + PF(\theta) \prec 0$   \\ Match desired poles by LMI
• Build $A_{sec}(\theta)$ and determine gain $K$ using eq(20 − 22)      \\ Extract feedback gain.
```

Remark: If the system is not block transformable, augmentation is performed as proposed by J.S. Shieh (see Malika Yaici [29,30]). For the application, let us consider the example presented in Fredriksson, J. [25], Yan, in [36], and Misgeld [46].

4. Representative Case Studies and Results

To assess the effectiveness and practical relevance of the proposed output feedback design, two representative case studies are presented. These examples illustrate the synthesis of feedback gain matrices under structural and spectral constraints, using block companion transformations and sector-based parameterization. Closed-loop pole placement is achieved through either an LMI-constrained framework or symbolic computation, depending on the structure of the sector matrix. The first example addresses blood gas regulation in extracorporeal circulation, which is a critical control problem in biomedical applications. The second example, presented later, highlights the method's generality and robustness.

Example 1: The regulation of patient blood gas levels within physiological ranges during stable extracorporeal circulation is a critical control problem [36], [46]. A schematic representation of the system configuration is shown in Fig. 1. The state and control variables are defined as follows: x_1 is oxygen flow rate, x_2 is carbon dioxide flow rate, x_3 is arterial partial pressure of oxygen (PaO2), x_4 is arterial partial pressure of carbon dioxide (PaCO2), u_1 is reference input for oxygen flow, and u_2 is reference input for carbon dioxide flow.

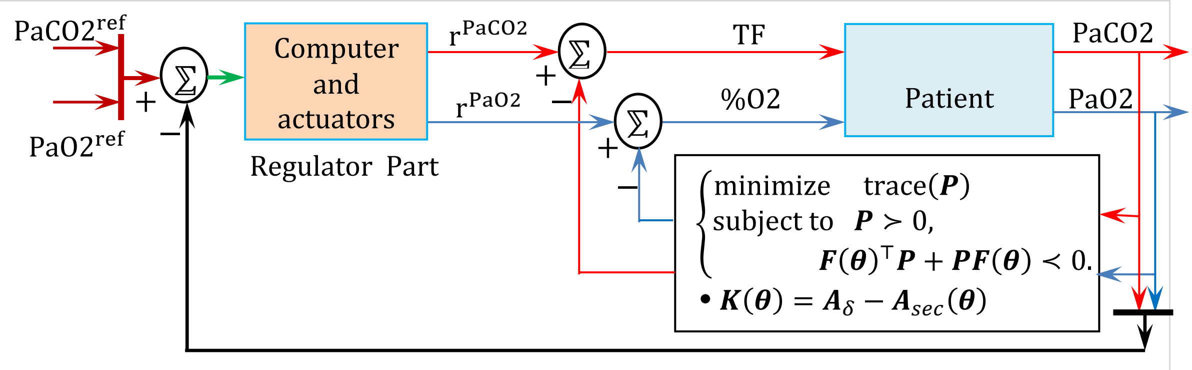

Fig. 1. Block diagram illustrating the control structure for patient blood gas regulation.

Consider a continuous-time state-space model whose parameters depend on the patient's condition. Nominal values can be estimated and stored for reference as needed. Based on typical data (see Magdi S. Mahmoud [41]), the model in equation (7) is defined by the matrices (A, B, C). The primary variables of interest are x_3 and x_4. Initially, the system's response is evaluated under a perturbation in arterial oxygen and carbon dioxide pressures. The state-space matrices are:

$$\left\{ \boldsymbol{A} = \begin{bmatrix} -10.045 & 0.002 & 0.003 & 0.001 \\ 0.0010 & -9.989 & 0.001 & 0.001 \\ 6.0450 & -3.002 & -4.997 & 0.001 \\ 0.0020 & 0.505 & 0.001 & -5.002 \end{bmatrix};\ \boldsymbol{B} = \begin{bmatrix} 10 & 0 \\ 0 & 10 \\ 0 & 0 \\ 0 & 0 \end{bmatrix};\ \boldsymbol{C} = \begin{bmatrix} 0 & 0 & 0 & 1 \\ 0 & 0 & 1 & 0 \end{bmatrix};\ \boldsymbol{D} = \boldsymbol{O}_{2\times 2} \right\}$$

Prior to implementing any control strategy, it is crucial to verify the system's asymptotic stability. In this application, stability will be enforced via output feedback. The corresponding block controllability and observability canonical transformations are defined as follows:

$$\left\{ \begin{array}{l} \boldsymbol{T}_{c1} = \boldsymbol{B}_c^\top \left[\text{row}\{\boldsymbol{A}^i\boldsymbol{B}\}_{i=0}^{\ell-1} \right]^{-1} = [\boldsymbol{O}_2 \ \ \boldsymbol{I}_2][\boldsymbol{B} \ \ \boldsymbol{AB}]^{-1} \\ \boldsymbol{T}_c = \text{col}\left(\boldsymbol{T}_{c1}\boldsymbol{A}^i\right)_{i=0}^{\ell-1} = \begin{bmatrix} \boldsymbol{T}_{c1} \\ \boldsymbol{T}_{c1}\boldsymbol{A} \end{bmatrix} \end{array} \middle| \begin{array}{l} \boldsymbol{T}_{o1} = \left[\text{col}\{\boldsymbol{C}\boldsymbol{A}^i\}_{i=0}^{\ell-1} \right]^{-1} \boldsymbol{C}_o^\top = \begin{bmatrix} \boldsymbol{C} \\ \boldsymbol{CA} \end{bmatrix}^{-1} \begin{bmatrix} \boldsymbol{O}_2 \\ \boldsymbol{I}_2 \end{bmatrix} \\ \boldsymbol{T}_o = \text{row}\left(\boldsymbol{A}^i\boldsymbol{T}_{o1}\right)_{i=0}^{\ell-1} = [\boldsymbol{T}_{o1} \ \ \boldsymbol{A}\boldsymbol{T}_{o1}] \end{array} \right\}$$

We now proceed to compute the matrix $\boldsymbol{A}_{co}$

$$\boldsymbol{A}_{co} = \boldsymbol{T}_c\boldsymbol{A}\boldsymbol{T}_o = \begin{bmatrix} 0.0981 & 0.0165 & -1.47640 & -0.2482 \\ 0.1976 & -0.0001 & -2.96260 & 0.0012 \\ -1.4764 & -0.2482 & 17.2798 & 2.9052 \\ -2.9626 & 0.0012 & 34.5366 & -0.0157 \end{bmatrix} = \begin{bmatrix} \boldsymbol{A}_\alpha & \boldsymbol{A}_\beta \\ \boldsymbol{A}_\gamma & \boldsymbol{A}_\delta \end{bmatrix}$$

The desired eigenvalues for the non-defective closed-loop system are given by $\lambda_{1,2} = -75597 \pm 124024i$ and $\lambda_{3,4} = -74568 \pm 129237i$. The corresponding characteristic polynomial is given by: $\Delta(\lambda) = \lambda^4 + 30\lambda^3 + 659\lambda^2 + 6512\lambda + 46967$. The parameterized desired matrix is:

$$\boldsymbol{A}_d = \boldsymbol{T}_c^{-1} \begin{bmatrix} 0.0981 & 0.0165 & -1.4764 & -0.2482 \\ 0.1976 & -0.0001 & -2.9626 & 0.0012 \\ -1.4764 & -0.2482 & \theta_{11} & \theta_{12} \\ -2.9626 & 0.0012 & \theta_{21} & \theta_{22} \end{bmatrix} \boldsymbol{T}_o^{-1} = \mathbf{F}(\boldsymbol{\theta}); \qquad \text{and} \qquad \boldsymbol{\theta} = \begin{bmatrix} \theta_{11} \\ \theta_{12} \\ \theta_{21} \\ \theta_{22} \end{bmatrix}$$

To enforce the sector matrix $\boldsymbol{A}_{sec}(\boldsymbol{\theta})$ to match the desired characteristic polynomial, we solve the following system of equations $\det\left(\lambda\boldsymbol{I} - \boldsymbol{A}_d(\boldsymbol{\theta})\right) = \Delta(\lambda) = \lambda^4 + 30\lambda^3 + 659\lambda^2 + 6512\lambda + 46967$ using the LMI-constrained framework. By using equations (20) and (21) we obtain the output feedback matrix

$$\boldsymbol{A}_{sec} = \begin{bmatrix} 0.6569 & 0.2920 \\ 0.6280 & 0.4317 \end{bmatrix} \qquad \Longrightarrow \qquad \boldsymbol{K} = \boldsymbol{A}_\delta - \boldsymbol{A}_{sec} = \begin{bmatrix} 16.6229 & 2.6132 \\ 33.9086 & -0.4473 \end{bmatrix}$$

Example 2: A fundamental component in power generation systems is the turbo-generator, illustrated in Figure 2. Its dynamic model comprises six state variables, two control inputs, and two measurable outputs (refer to [32], [47], and [48])

The input u_1 is the turbine throttle (steam valve) and is typically used to control y_1: the generator terminal voltage (GTV), while the input u_2 is the excitation voltage (field current input) that controls y_2: the electrical active power output (EAP) of the generator. Both the GTV and EAP paths are dynamically coupled through the electromechanical interaction between the turbine and the synchronous generator, constituting an inherently multivariable control problem as depicted in Fig. 2. The goal is to track GTV/EAP setpoints in the presence of load and frequency disturbances using steam valve and excitation positions. Using appropriate data see (Magdi S. Mahmoud [41]), the system matrices are given by:

$$\boldsymbol{A} = \begin{bmatrix} -18.4456 & 4.2263 & -2.2830 & 0.2260 & 0.4220 & -0.0951 \\ -4.09770 & -6.0706 & 5.6825 & -0.6966 & -1.2246 & 0.2873 \\ 1.4449 & 1.4336 & -2.6477 & 0.6092 & 0.8979 & -0.2300 \\ -0.00930 & 0.2302 & -0.5002 & -0.1764 & -6.3152 & 0.1350 \\ -0.04640 & -0.3489 & 0.7238 & 6.3117 & -0.6886 & 0.3645 \\ -0.06020 & -0.2361 & 0.2300 & 0.0915 & -0.3214 & -0.2087 \end{bmatrix}; \quad \boldsymbol{B} = \begin{bmatrix} -0.2748 & 3.14630 \\ -0.0501 & -9.37370 \\ -0.1550 & 7.42906 \\ 0.0716 & -4.91760 \\ -0.0814 & -10.2648 \\ 0.0244 & 13.7943 \end{bmatrix}$$

$$\boldsymbol{C}=\begin{bmatrix}0.5971 & -0.7697 & 4.8850 & 4.8608 & -9.8177 & -8.86100\\ 3.1013 & 9.3422 & -5.6000 & -0.7490 & 2.9974 & 10.5719\end{bmatrix};\quad \boldsymbol{D}=\boldsymbol{O}_{2\times 2}$$

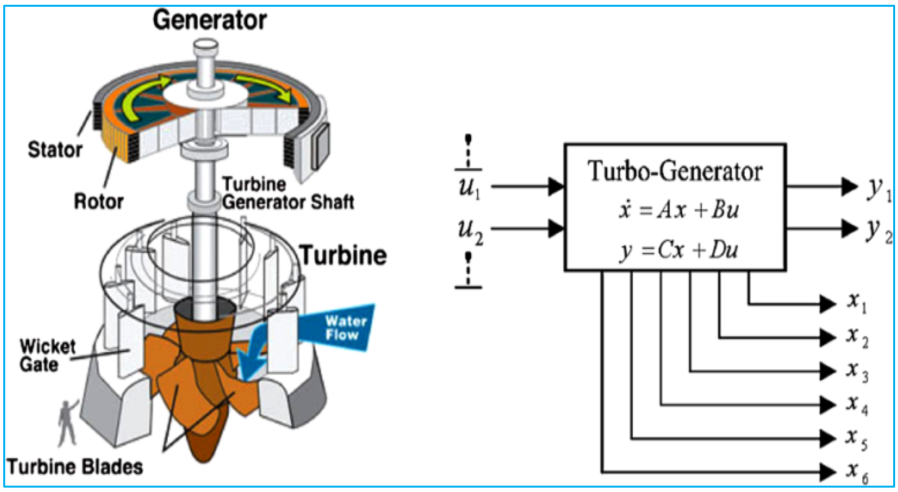

Fig. 2. Turbo-generator system: physical configuration and corresponding block diagram.

The turbo-generator system defined by $(\boldsymbol{A},\boldsymbol{B},\boldsymbol{C},\boldsymbol{D})$ is block controllable with a controllability index $\ell=n/m=3$, and block observable with an observability index $v=n/p=3$. The objective is to determine an output feedback gain matrix that assigns the next self-conjugate eigenvalues: $\lambda_1=-19.6462$, $\lambda_{2,3}=-28375\pm 93511i$, $\lambda_{4,5}=-10131\pm 56009i$ and $\lambda_6=-0.8293$. Therefore: $\Delta(\lambda)=\lambda^6+28\lambda^5+313\lambda^4+3357\lambda^3+13091\lambda^2+69493\lambda+50404$. The block controllability and observability transformation matrices are given by:

$$\left\{\begin{array}{l|l} \boldsymbol{T}_{c1}=\boldsymbol{B}_c^{\top}\left[\mathrm{row}\{\boldsymbol{A}^i\boldsymbol{B}\}_{i=0}^{\ell-1}\right]^{-1}=[\boldsymbol{O}_2\ \boldsymbol{I}_2][\boldsymbol{B}\ldots\boldsymbol{A}^2\boldsymbol{B}]^{-1} & \boldsymbol{T}_{o1}=\left[\mathrm{col}\{\boldsymbol{C}\boldsymbol{A}^i\}_{i=0}^{\ell-1}\right]^{-1}\boldsymbol{C}_o^{\top}=\begin{bmatrix}\boldsymbol{C}\\ \boldsymbol{C}\boldsymbol{A}\\ \boldsymbol{C}\boldsymbol{A}^2\end{bmatrix}^{-1}\begin{bmatrix}\boldsymbol{O}_2\\ \boldsymbol{O}_2\\ \boldsymbol{I}_2\end{bmatrix}\\ \boldsymbol{T}_c=\mathrm{col}\left(\boldsymbol{T}_{c1}\boldsymbol{A}^i\right)_{i=0}^{\ell-1}=\begin{bmatrix}\boldsymbol{T}_{c1}\\ \boldsymbol{T}_{c1}\boldsymbol{A}\\ \boldsymbol{T}_{c1}\boldsymbol{A}^2\end{bmatrix} & \boldsymbol{T}_o=\mathrm{row}\left(\boldsymbol{A}^i\boldsymbol{T}_{o1}\right)_{i=0}^{\ell-1}=[\boldsymbol{T}_{o1}\ \ \boldsymbol{A}\boldsymbol{T}_{o1}\ \ \boldsymbol{A}^2\boldsymbol{T}_{o1}] \end{array}\right\}$$

The matrix obtained after applying the left and right similarity transformations is given by:

$$\boldsymbol{A}_{co}=\begin{bmatrix}-0.0018 & 0.0001 & 0.0842 & -0.0042 & -0.0494 & 0.1502\\ 0.0001 & -0.0000 & -0.0079 & 0.0003 & 0.0083 & -0.0100\\ 0.0842 & -0.0042 & -0.0494 & 0.1502 & -4.2422 & -5.6939\\ -0.0079 & 0.0003 & 0.0083 & -0.0100 & 0.3768 & 0.4426\\ -0.0494 & 0.1502 & -4.2422 & -5.6939 & 30.7163 & 124.2214\\ 0.0083 & -0.0100 & 0.3768 & 0.4426 & -2.6304 & -10.0203\end{bmatrix}$$

$$\boldsymbol{A}_{co}=\boldsymbol{T}_c\boldsymbol{A}\boldsymbol{T}_o\qquad\Rightarrow\qquad \boldsymbol{A}_{\delta}=\boldsymbol{A}_{co}(5{:}6,5{:}6)=\begin{bmatrix}30.7163 & 124.2214\\ -2.6304 & -10.0203\end{bmatrix}$$

By matching the coefficients of the resulting characteristic polynomial with those of the desired one, i.e., ensuring det$\det\left(\lambda\boldsymbol{I}-\boldsymbol{A}_d(\boldsymbol{\theta})\right)=\boldsymbol{\Delta}(\lambda)$, a nonlinear system of equations is formed. Solving this system via a symbolic LMI-constrained optimization procedure yields the optimal output feedback matrix that ensures the specified closed-loop performance.

$$\boldsymbol{A}_{sec}(\boldsymbol{\theta})=\begin{bmatrix}30.7064 & 124.1879\\ -2.6566 & -10.0883\end{bmatrix}\quad\Longrightarrow\quad \boldsymbol{K}(\boldsymbol{\theta})=\boldsymbol{A}_{\delta}-\boldsymbol{A}_{sec}(\boldsymbol{\theta})=\begin{bmatrix}0.0099 & 0.0335\\ 0.0262 & 0.0680\end{bmatrix}$$

By exploiting the structural features of parametric vectorized companion forms, a unified framework was established to derive closed-form expressions for output feedback controllers with nonlinear parameterization, enabling arbitrary eigenvalue assignment in linear multivariable systems that are block-controllable and block-observable. It was shown that the feedback gain can consistently be computed using the equation (21), where the associated parameters are systematically determined by solving a nonlinear system of equations. Importantly, the proposed approach does not rely on knowledge of the open-loop spectrum and places no constraints on the location, type, or multiplicity of the desired eigenvalues.

5. Comparison Using the Turbo-Generator Case Study

The proposed output feedback controller is evaluated alongside two established methods: adaptive pole placement and eigenstructure assignment via Moore's algorithm. Each technique was applied to the linearized MIMO turbo-generator system. While all methods achieved closed-loop stability and acceptable dynamic response, the proposed design consistently outperformed in terms of spectral robustness, sensitivity attenuation, and reduced control effort. Simulation results (Fig. 3 and Fig. 4) confirm that the proposed method ensures smooth regulation with minimal error, while the other methods incur higher overshoot, input effort, or sensitivity. All simulations were conducted using MATLAB R2023a on a Windows 10 64-bit system, equipped with an Intel Core i7-1165G7 CPU @ 2.80GHz and 16 GB of RAM.

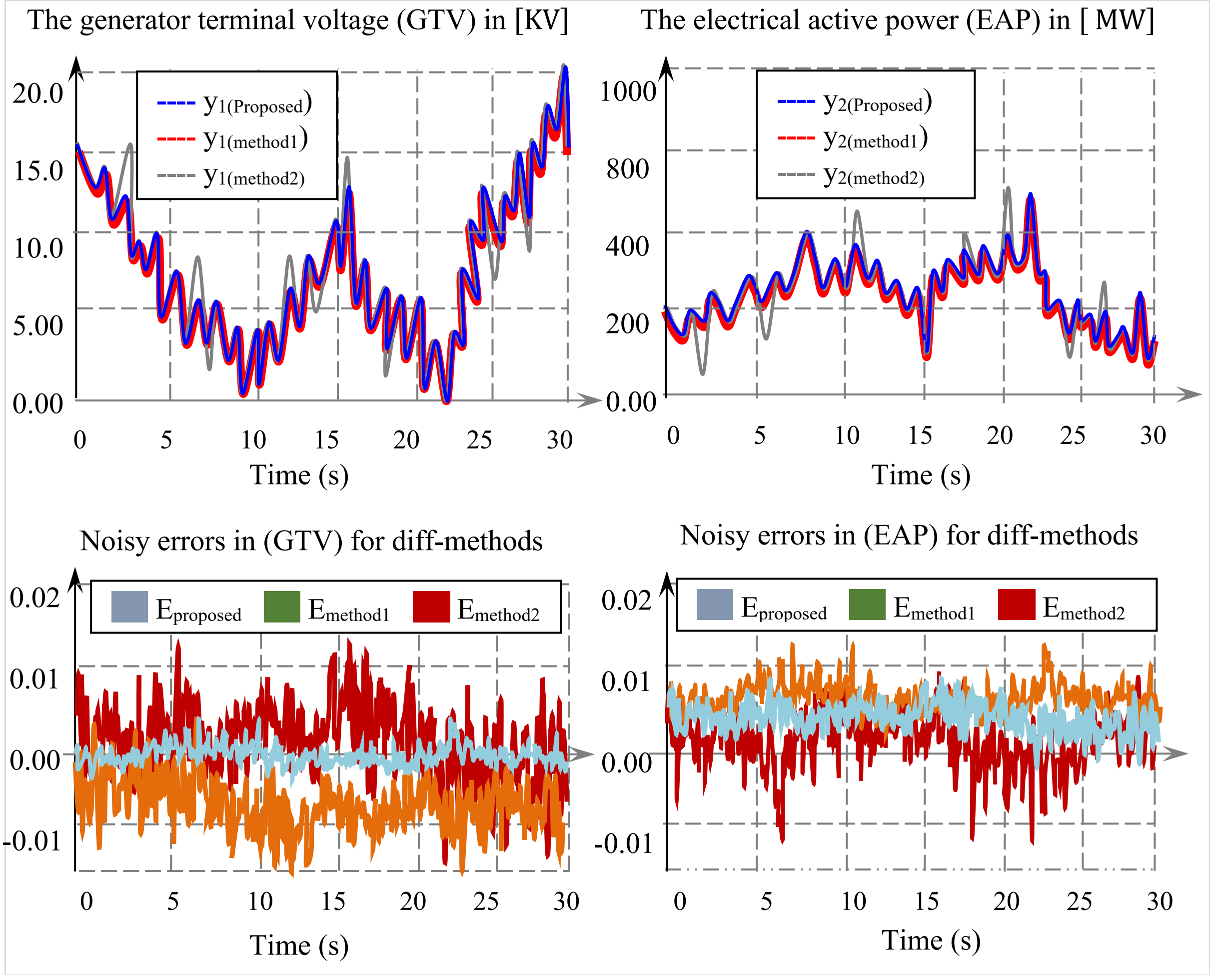

Fig. 3. Test results of GTV and EAP set points tracking for the turbo-generator.

The sensitivity of the i^{th} eigenvalue of a closed-loop matrix $\boldsymbol{A}$ to perturbations is given by:

√ Let λ and $\hat{\lambda}$ be the eigenvalues of $\boldsymbol{A}$ and $\boldsymbol{A}+\Delta\boldsymbol{A}$ respectively, and $\boldsymbol{V}$ is the right eigenvectors matrix of $\boldsymbol{A}$, then $\kappa(\boldsymbol{V}) \geq \min_{i}\{\lambda_i - \hat{\lambda}_i\}/\|\Delta\boldsymbol{A}\|$ where $\kappa(.)$ the condition number.

√ Let λ_i, $\mathbf{v}_i$ and $\boldsymbol{t}_i$ be the i^{th} eigenvalue, right and left eigenvectors of $\boldsymbol{A}$, respectively, and let $\lambda_i + \Delta\lambda_i$ be the i^{th} eigenvalue of $\boldsymbol{A}+\Delta\boldsymbol{A}$ $(i = 1, 2, \ldots, n)$. Then: $s(\lambda_i) = \|\boldsymbol{t}_i\| \,.\, \|\mathbf{v}_i\| \geq \Delta\lambda_i/\|\Delta\boldsymbol{A}\|$.

√ The individual relative change in eigenvalues is $r_i = r(\lambda_i) = |\Delta\lambda_i|/|\lambda_i|$ for $i = 1, 2, \ldots, n$.

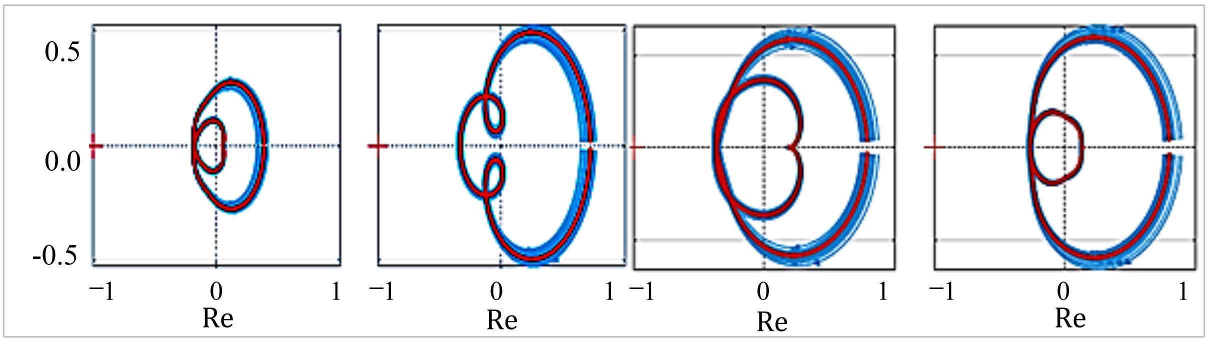

Fig. 4. Nyquist diagram of the closed loop system of the turbo-generator.

The robustness and spectral sensitivity of the proposed output feedback gain design is evaluated by analyzing the perturbation behavior of the closed-loop eigenstructure. The sensitivity, condition number, and relative eigenvalue variations are computed for each method. The following tables (Table 1, Table 2, Table 3, Table 4) summarize the comparative performance in terms of eigenvalue displacement bounds, spectral conditioning, and robustness under norm-bounded perturbations.

Table 1. The gain matrices and the associated norms for the turbo-generator system

Methods	$\|\boldsymbol{K}\|_{\mathrm{F}}$	$\|\boldsymbol{K}\|_2$	$\|\boldsymbol{K}\|_{\max}$	$\|\boldsymbol{K}\|_\infty$	$\|\boldsymbol{K}\|_1$	$\|\boldsymbol{H}(j\omega)\|_\infty$
Tong Ma et.al [38]	6.4382	3.8601	2.7903	6.9202	6.7105	4.9852
Talha M et.al [40]	5.7324	3.2725	2.3341	6.1189	5.9803	4.1167
Proposed	0.0808	0.0785	0.0680	0.0942	0.1015	2.1984

- The feedback gain norms $\|\boldsymbol{K}\|_\star$ for the proposed method are orders of magnitude smaller (e.g., $\|\boldsymbol{K}\|_{\mathrm{F}} = 0.0808$) compared to [38] (6.4382) or [40] (5.7324). This clearly reflects the effectiveness of the sector matrix parameterization, which yield a minimal-energy controller.
- The $\|\boldsymbol{H}(j\omega)\|_\infty$ values confirm superior frequency robustness of the proposed method, with lower gain peaking (2.1984 vs. 4.9852), ensuring better disturbance rejection and stability margins. This validates the effectiveness of the LMI-based pole placement in yielding a well-conditioned feedback loop.

Table 2. Time-domain performance comparison using different methods

Methods	Settling time (s)	Overshoot [%]		Max-efforts		Error	
		y_1	y_2	$\{\mathrm{In}_1\}_{\max}$	$\{\mathrm{In}_2\}_{\max}$	$\{e_1\}_{\max}$	$\{e_2\}_{\max}$
Tong Ma et.al [38]	0.93	1.3	0.1	35.20	04.18	0.03	0.01
Talha M et.al [40]	1.42	4.6	0.4	13.25	22.5	0.21	0.12
Proposed	1.88	5.2	0.8	14.12	3.12	0.013	0.009

The comparison of transient behaviors across control strategies reveals key differences in trade-offs between speed, effort, and accuracy.

- The method of [38] achieves the fastest settling time (0.93 s) and lowest overshoot (1.3%), which indicates aggressive response shaping. However, this comes at the cost of very high control effort, particularly on input In_1 (35.20), and moderate error magnitudes.
- The method of the reference [40] trikes a middle ground in control effort but suffers from increased overshoot (4.6%) and slower settling (1.42 s). Additionally, the tracking errors $e_{1\max} = 0.21$, $e_{2\max} = 0.12$ are higher than desired, especially under disturbance.
- The proposed method yields smooth control with very low tracking error ($e_{1\max} = 0.013$, $e_{2\max} = 0.009$), outperforming both alternatives in steady-state accuracy. Although it has a longer settling time (1.88 s), it offers strong robustness and minimal control saturation—key advantages in noisy or uncertain environments. Time-domain results (Figure 3) confirm stable convergence without overshoot or actuator peaking.

Table 3. Robust stability (Eigenvalues sensitivity $s(.)$)

Methods	$s(\lambda_1)$	$s(\lambda_2)$	$s(\lambda_3)$	$s(\lambda_4)$	$s(\lambda_5)$	$s(\lambda_6)$
Tong Ma et.al [38]	4.4123	5.2016	6.8710	3.9184	4.6722	5.7391
Talha M et.al [40]	3.9425	4.7213	5.4822	3.2215	4.0051	4.8936
Proposed	2.1189	2.4928	3.1436	1.8047	2.2104	2.7520

- The sensitivity values $s(\lambda_i)$ quantify how sensitive each eigenvalue is to perturbations. Again, the proposed method yields the lowest values across all modes (e.g., $s(\lambda_3) = 3.1436$ vs. 6.8710 for Tong Ma [38]), indicating a tightly clustered and robust spectrum.
- This is a direct consequence of the structured output-feedback realization and sector matrix shaping, which keeps the eigenstructure stable and resilient to parameter drift.

These results confirm that the proposed method significantly enhances spectral robustness, offering better resistance to eigenvalue perturbations compared to existing approaches.

Table 4. Robust performance (Relative change r in the eigenvalues, under perturbation)

Methods	$r(\lambda_1)$	$r(\lambda_2)$	$r(\lambda_3)$	$r(\lambda_4)$	$r(\lambda_5)$	$r(\lambda_6)$
Tong Ma et. al [38]	0.0923	0.1147	0.1315	0.0796	0.1051	0.1284
Talha M et. al [40]	0.0612	0.0748	0.0893	0.0527	0.0690	0.0832
Proposed	0.0185	0.0251	0.0339	0.0152	0.0208	0.0286

- The relative eigenvalue displacements $r(\lambda_i)$ under perturbations are drastically reduced in the proposed method (e.g., 0.0185 vs. 0.0923 for Tong Ma [38]). This indicates a high spectral robustness — the closed-loop poles remain nearly unchanged even under system perturbations.
- For safety-critical or grid-connected turbo-generator systems, such resilience ensures predictable behavior during faults or transients, which is crucial for fault-tolerant operation.

The proposed output feedback gain design notably enhances control performance by reducing control effort, improving steady-state accuracy, increasing spectral robustness, and attenuating sensitivity to disturbances. As illustrated in Fig. 4, the Nyquist plot confirms closed-loop stability. Since the open-loop system is stable ($P = 0$), the Nyquist contour Γ_c mapped by $\boldsymbol{H}_{\text{sys}}\left(e^{j\omega T_s}\right)$ does not encircle the critical point $(-1,0)$, satisfying the condition $Z = N = 0$. This guarantees the internal stability of the system. All of this is achieved without compromising stability, as verified both numerically (Table 1, Table 2, Table 3, Table 4) and graphically (system response plots in Fig. 3 and Fig. 4). The method's reliance on sector decomposition and LMI optimization proves highly effective, offering a structured yet flexible framework for modern MIMO control design.

To better highlight the comparative effectiveness of the three control strategies, their performance is assessed using the root-mean-squared error (RMSE) and the integral of squared error (ISE). As shown in Fig. 5, the proposed controller achieves significantly lower RMSE values of $(0.0137,\ 0.0110)$ and ISE values of $(0.4560,\ 0.1800)$. These results confirm the superior tracking precision of the proposed method compared to the two benchmark approaches.

The 3D performance visualizations clearly highlight the superiority of the proposed method across both output channels. As shown in the RMSE and ISE plots, the proposed controller achieves the lowest error magnitudes for y_1 and y_2, significantly outperforming the methods of Tong Ma and Talha M. The consistent reduction in both RMSE and ISE reflects the enhanced steady-state accuracy and efficient disturbance rejection of the proposed LMI-based design. Additionally, the color-coded bars per method emphasize the clear advantage in overall performance robustness.

6. Conclusion and Directions for Future Work

This paper has presented a novel and efficient output feedback design framework for multivariable systems, based on a parametric formulation that leverages block controllability and observability transformations. Unlike traditional methods relying on iterative tuning, prior state feedback, or restrictive assumptions, the proposed approach enables direct closed-loop pole placement via sector matrix parameterization solved through LMI optimization. Numerical results on a turbo-generator system confirm its advantages in precision, control effort, and robustness to spectral perturbations, consistently outperforming conventional techniques in accuracy, stability, and computational efficiency. The method is also readily implementable in LMI-based environments such as MATLAB, with fast offline computation using solvers like SeDuMi or MOSEK. For medium-scale MIMO systems (state dimension ≤ 20), execution time remains below one second, and the static gain matrix ensures suitability for real-time and embedded applications. These findings position the approach as a reliable and scalable solution for high-performance MIMO control in practical settings.

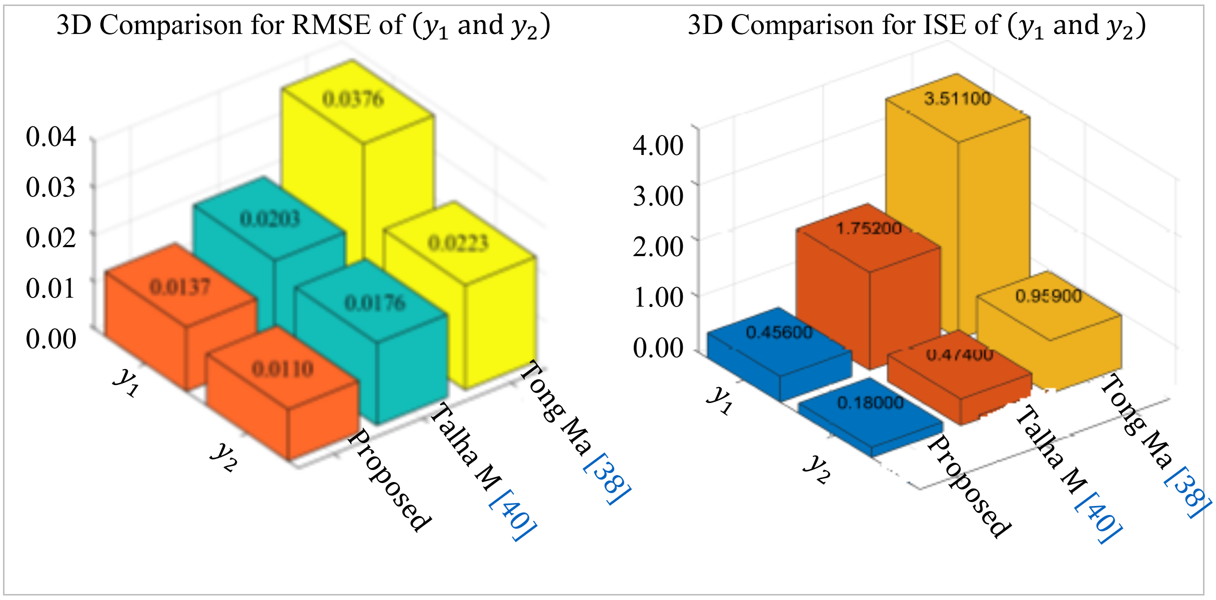

Fig. 5. The performance comparison of three control methods using RMSE and ISE.

Recent developments in artificial intelligence and optimization have opened new possibilities for addressing complex nonlinear control problems. Techniques such as Physics-Informed Neural Networks (PINNs), Genetic Algorithms (GAs), and Particle Swarm Optimization (PSO) offer powerful frameworks for global search, model learning, and data-driven decision-making. The combination of deep learning with numerical computation is particularly promising for enhancing convergence, adaptability, and real-time responsiveness in modern control systems. Building on the current results, the following directions are suggested for future exploration:

1. **Integration of Hybrid AI and Classical Controls**: Future work may combine deep learning, such as Physics-Informed Neural Networks, with classical control to create robust, adaptive solutions for nonlinear systems.
2. **Scalability to Large-Scale MIMO Systems**: Extending AI-based methods to high-dimensional MIMO systems could reveal their robustness and scalability, especially in robotics and autonomous vehicles.
3. **Real-time Adaptation and Learning**: Further investigation into reinforcement learning and adaptive neural control techniques could enable controllers that adjust in real-time to system variations, potentially improving performance in environments with changing dynamics or incomplete models.
4. **Improving Optimization Efficiency**: Enhancing the speed and scalability of learning-based optimizers through parallel computing, GPU acceleration, and hybrid solvers remains a key challenge for real-time deployment.
5. **Experimental Validation**: Practical validation of AI-enhanced controllers on physical platforms such as robotic manipulators, drones, or industrial processes would provide important feedback, helping bridge theoretical advancements with real-world performance.

These future directions aim to extend the proposed framework into more adaptive, scalable, and experimentally validated solutions, reinforcing its potential as a foundation for next-generation intelligent multivariable control systems.

Author Contribution: All authors contributed equally to the main contributor to this paper. All authors read and approved the final paper.

Funding: This research received no external funding.

Conflicts of Interest: The authors declare no conflict of interest.

References

[1] T. Topaloglu and D. E. Seborg, “A design procedure for pole assignment using output feedback,” *Int. J. Control*, vol. 22, no. 6, pp. 741-748, 1975, https://doi.org/10.1080/00207177508922119.

[2] E. Davison and S. Wang, “On pole assignment in linear MIMO systems using output feedback,” *IEEE Trans. Automat. Control*, vol. 20, pp. 516–518, 1975, https://doi.org/10.1109/TAC.1975.1101023.

[3] H. Kimura, “Pole assignment by gain output feedback,” *IEEE Trans. Automat. Control*, vol. 20, no. 4, pp. 509–516, 1975, https://doi.org/10.1109/TAC.1975.1101028.

[4] L. R. Fletcher and J. F. Magni, “Exact pole assignment by output feedback Part 1*,” Int. J. Control*, vol. 45, no. 6, pp. 1995-2007, 1987, https://doi.org/10.1080/00207178708933862.

[5] J. C. Willems and W. H. Hesselink, “Generic properties of the pole placement problem,” *IFAC Proceedings Volumes*, vol. 11, no. 1, pp. 1725-1729, 1978, Helsinki, 1978, https://doi.org/10.1016/S1474-6670(17)66142-1.

[6] R. Hermann and C. F. Martin, “Applications of algebraic geometry to system theory Part I,” *IEEE Trans. Automat. Control*, vol. 22, no. 1, pp. 19–25, 1977, https://doi.org/10.1109/TAC.1977.1101395.

[7] J. Kautsky, N. K. Nichols, and P. Van Dooren, “Robust pole assignment in linear state feedback,” *Int. J. Control*, vol. 41, no. 5, pp. 1129–1155, 1985, https://doi.org/10.1080/0020718508961188.

[8] A. N. Andry, E. Y. Shapiro, and J. C. Chung “Eigenstructure assignment for linear systems,” *IEEE Trans. Aerosp. Electron. Syst.*, vol. 19, no. 5, pp. 711–729, 1983, https://doi.org/10.1109/TAES.1983.309373.

[9] L. Carotenuto and G. Franze, “A general formula for eigenvalue assignment by static output feedback,” *Systems Control Letters*, vol. 49, no. 3, pp. 175–190, 2003, https://doi.org/10.1016/S0167-6911(02)00321-3.

[10] E. K. Chu, “Optimization and pole assignment in control system design,” *Int. J. Appl. Math. Comput.*, vol. 5, 1035–1053, 2001, http://eudml.org/doc/207544.

[11] C. Champetiert and J. -F. Magni, “On Eigenstructure Assignment by Gain Output Feedback,” *SIAM J. Control and Optimization*, vol. 29, No. 4, pp. 848–865, 1991, https://doi.org/10.1137/0329046.

[12] G. Roppeneeker and J. O’Reilly, “Parametric output feedback controller design,” *Automatica*, vol. 25, no. 2, pp. 259-265, 1989, https://doi.org/10.1016/0005-1098(89)90079-4.

[13] L. S. Shieh and Y. T. Tsay, “Block modal matrices and their applications to multivariable control systems,” *IEE Proceedings D (Control Theory and Applications)*, vol. 129, no. 2, pp. 41–48, 1982, https://doi.org/10.1049/ip-d.1982.0010.

[14] L. S. Shieh and Y. T. Tsay, “Transformation of multivariable systems to block companion forms,” *Computers and Mathematics with Applications*, vol. 14, no. 6, pp. 471-477, 1987, https://doi.org/10.1016/0898-1221(87)90059-9.

[15] L. S. Shieh and Y. T. Tsay, “Transformation of solvent and spectral factors,” *Int. J. Control*, vol. 34, no. 4, pp. 813–823, 1981, https://doi.org/10.1080/00207178108922562.

[16] T. Kailath, *Linear Systems*, Prentice-Hall, New Jersey, 1980, https://books.google.co.id/books?id=ggYqAQAAMAAJ.

[17] D. Jiang and J. Wang, “Augmented gradient flows for on-line robust pole assignment via state and output feedback,” *Automatica J. Control*, vol. 38, no. 2, pp. 279–286, 2002, https://doi.org/10.1016/S0005-1098(01)00200-X.

[18] E. A. Galperin, “Outline of new algorithm for output feedback pole placement,” *Proc. IEEE Int. Symp. on Computer-Aided Control System Design*, pp. 60–64, 2000, https://doi.org/10.1109/CACSD.2000.900187.

[19] S. M. Karbassi and F. Saadatjou, “A parametric approach for eigenvalue assignment by static output feedback,” *Journal of the Franklin Institute*, vol. 346, no. 4, pp. 289–300, 2009, https://doi.org/10.1016/j.jfranklin.2008.10.001.

[20] B. Bekhiti, “On λ-matrices and their applications in MIMO control systems design,” *Int. J. Modelling, Identification and Control*, vol. 29, no. 4, pp 281-294, 2018, https://doi.org/10.1504/IJMIC.2018.092115.

[21] B. Bekhiti and K. Hariche, “Block-Structure Relocation via State and State Derivative Feedback,” *Journal of Control and Systems Engineering*, vol. 4, no. 1, pp. 95–111, 2016, https://doi.org/10.18005/JCSE0401010.

[22] B. Bekhiti and A. Dahimene, “On the theory of λ-matrices based MIMO control system design,” *Control and Cybernetics*, vol. 44, no. 4, pp. 421–443, 2015, https://yadda.icm.edu.pl/baztech/element/bwmeta1.element.baztech-24cfdc21-13c1-4247-8199-7979c921f52b.

[23] I. Gohberg, P. Lancaster, and L. Rodman, *Matrix Polynomials*, Academic Press, 1982, https://books.google.co.id/books?id=KwEItnMvwbgC.

[24] S. M. Karbassi and H. A. Tehrani, “Parameterizations of the state feedback controllers for linear multivariable systems,” *Comput. Math. Appl.*, vol. 44, no. 8, pp. 1057–1065, 2002, https://doi.org/10.1016/S0898-1221(02)00214-6.

[25] J. Fredriksson and B. Egardt, “Backstepping control with local LQ performance,” *Proc. 40th IEEE CDC*, vol. 1, pp. 111–116, 2001, https://doi.org/10.1109/CDC.2001.980081.

[26] A. Ichikawa and H. Katayama, “The design of deadbeat controllers by state transition graph,” *IEEE Trans. Automat. Control*, vol. 36, no. 6, pp. 752–756. 2002, https://doi.org/1991. 10.1109/9.86951.

[27] K. Hariche and E. D. Denman, “On interpolation theory and λ-matrices,” *J. Math. Anal. Appl.*, vol. 143, no. 2, pp. 530–547, 1989, https://doi.org/10.1016/0022-247X(89)90058-9.

[28] B. Bekhiti, A. Dahimene, B. Nail, K. Hariche, and A. Hamadouche, “On Block Roots of Matrix Polynomials Based MIMO Control System Design,” *4th IEEE Int. Conf. on Electrical Engineering (ICEE)*, Boumerdes, 2015, https://doi.org/10.1109/INTEE.2015.7416694.

[29] M. Yaici and K. Hariche, “On eigenstructure assignment using Block poles placement,” *European Journal of Control*, Vol 20, No 5, pp. 217–226, 2014, https://doi.org/10.1016/j.ejcon.2014.05.003.

[30] M. Yaici, K. Hariche, and C. Tim “A Contribution to the Polynomial Eigen Problem,” *Int. J. of Mathematics, Computational, Natural and Physical Engineering*, vol. 8, no. 10, 2014, https://doi.org/10.5281/zenodo.1096463.

[31] B. Bekhiti, A. Dahimene, K. Hariche, *Advanced Nonlinear Control and State Observation in Robotics*, Scholars’ Press, 2017, https://books.google.co.id/books?id=ysiAtAEACAAJ.

[32] M. Jung, K. Glover, and U. Christen “Comparison of Uncertainty Parameterizations for H∞ Robust Control of Turbo charged Diesel Engines,” *Control Engineering Practice*, vol. 13, no. 1, pp. 15-25, 2005, https://doi.org/10.1016/j.conengprac.2003.12.018

[33] K. B. Slimane, Z. Tmar, and M. Besbes, "Deep reinforcement learning LQR controller design for MIMO systems," *Int Journal of Automation and Control*, vol. 19, no. 1, 2025, https://doi.org/10.1504/IJAAC.2025.10067319.

[34] B. Bekhiti, J. Iqbal, K. Hariche, and G. F. Fragulis, "Neural Adaptive Nonlinear MIMO Control for Bipedal Walking Robot Locomotion in Hazardous and Complex Task Applications," *Robotics*, vol. 14, no. 6, p. 84, 2025, https://doi.org/10.3390/robotics14060084.

[35] L.-B. Wu, J. H. Park, X. -P. Xie, and Y. -J. Liu "Neural Network Adaptive Tracking Control of Uncertain MIMO Nonlinear Systems With Output Constraints and Event-Triggered Inputs," *IEEE Trans. Neural Networks Learn. Syst.*, vol. 32, no. 2, pp. 695-707, 2020, https://doi.org/10.1109/TNNLS.2020.2979174.

[36] Z. Yan, Z. Zhang, G. Hu, and B. Zhu, "Observer-Based Finite-Time H∞ Control of the Blood Gases System in Extracorporeal Circulation via the T-S Fuzzy Model," *Mathematics*, vol. 10, no. 12, p. 2102, 2022, https://doi.org/10.3390/math10122102.

[37] A. Rauh and S. Romig "Linear Matrix Inequalities for an Iterative Solution of Robust Output Feedback Control of Systems with Bounded and Stochastic Uncertainty," *Sensors*, vol. 21, no. 9, p. 3285, 2021, https://doi.org/10.3390/s21093285.

[38] T. Ma, "Eigenvalue assignment enabled control law for multivariable nonlinear systems with mismatched uncertainties," *European Journal of Control*, vol. 56, no. 1, pp. 154-166, 2020, https://doi.org/10.1016/j.ejcon.2020.03.002

[39] T. Ma and C. Cao, "L1 adaptive output-feedback control of multivariable nonlinear systems subject to constraints using online optimization," *Int. J. Robust Nonlinear Control*, vol. 29, no. 12, pp. 4116-4134, 2019, https://doi.org/10.1002/rnc.4597.

[40] T. Mushtaq, P. Seiler, and M. S. Hemati, "On the convexity of static output feedback control synthesis," *Automatica*, vol. 159, p. 111380, 2024, https://doi.org/10.1016/j.automatica.2023.111380.

[41] M. S. Mahmoud and Y. Xia, *Applied Control Systems Design*, Springer, 2012, https://books.google.co.id/books?id=MPAQkwFiMhoC.

[42] G. Cai, C. Hu, and G. Duan, "Eigenstructure assignment for linear parameter-varying systems with applications," *Math. and Comp. Modeling*, vol. 53, no. 5, pp. 861–870, 2011, https://doi.org/10.1016/j.mcm.2010.10.02.

[43] B. Bekhiti, B. Nail, I. E. Tibermacine, and R. Salim, "On Hyper-Stability Theory Based Multivariable Nonlinear Adaptive Control," *IET Electric Power Applications*, vol. 19, no. 1, p. e70035, 2025, https://doi.org/10.1049/elp2.70035.

[44] B. Bekhiti, G. F. Fragulis, M. Rahmouni, and K. Hariche, "A Novel Three-Dimensional Sliding Pursuit Guidance and Control of Surface-to-Air Missiles," *Technologies*, vol. 13, no. 5, p. 171, 2025, https://doi.org/10.3390/technologies13050171.

[45] B. Bekhiti, *Advanced Strategies for Guidance & Control of SAM Missiles*, Lambert, 2024.

[46] B. J. E. Misgeld, J. Werner, and M. Hexamer, "Robust and self-tuning blood flow control during extracorporeal circulation in the presence of system parameter uncertainties," *Medical & Biological Eng & Computing*, vol. 43, no. 5, pp. 589–598, 2005, https://doi.org/10.1007/BF02351032.

[47] W. Haiyan and J. Zhang "Control Oriented Dynamic Modeling of a Turbocharged Diesel Engine," *Sixth International Conference on Intelligent Systems Design and Applications (6th ISDA)*, 2006, https://doi.org/10.1109/ISDA.2006.253821.

[48] I. Friedrich, C. S. Liu, and D. Oehlerking "Coordinated EGR-rate model-based controls of turbocharged diesel engines via an intake throttle and an EGR valve," *IEEE Conf. on Vehicle Propulsion,* pp. 340–347, 2009, https://doi.org/10.1109/VPPC.2009.5289828.

[49] C. T. Chen, *Linear System Theory and Design*, Holt, Reinhart and Winston, 1984, https://books.google.co.id/books?id=HAJRAAAAMAAJ.

[50] S. Srinathkumar, "Eigenvalue/eigenvector assignment algorithm using output feedback," *IEEE Trans on Automatic Control*, vol. 23, no. 1, 1978, https://doi.org/10.1109/TAC.1978.1101685.

[51] B. Bekhiti, *Multivariable Control System Design Using the Theory of Matrix Polynomials*, PhD thesis, University of M'HAMED BOUGARA-Boumerdes (Algeria) 2018, https://www.ccdz.cerist.dz/admin/notice.php?id=00000000000000861226000621.

[52] K. Hariche and E. D. Denman, "On solvents and Lagrange interpolating λ-matrices," *Applied Math. Comput.*, vol. 25, no. 4, pp. 321-332, 1988, https://doi.org/10.1016/0096-3003(88)90127-0.